NASA TECHNICAL MEMORANDUM

NASA TM X-64873

ORBITER/SPACELAB MOMENTUM MANAGEMENT FOR POP ORIENTATIONS

By Jerry W. Cox
Systems Dynamics Laboratory

June 21, 1974

NASA

George C. Marshall Space Flight Center

Marshall Space Flight Center, Alabama

TECHNICAL REPORT STANDARD TITLE PAGE

1. REPORT NO.	2. GOVERNMENT ACCESSION NO.	3. RECIPIENT'S CATALOG NO.
NASA TM X- 64873		

4. TITLE AND SUBTITLE	5. REPORT DATE
Orbiter/Spacelab Momentum Management for POP Orientations	June 21, 1974
	6. PERFORMING ORGANIZATION CODE

7. AUTHOR(S)	8. PERFORMING ORGANIZATION REPORT #
Jerry W. Cox	

9. PERFORMING ORGANIZATION NAME AND ADDRESS	10. WORK UNIT NO.
George C. Marshall Space Flight Center Marshall Space Flight Center, Alabama 35812	11. CONTRACT OR GRANT NO.
	13. TYPE OF REPORT & PERIOD COVERED

12. SPONSORING AGENCY NAME AND ADDRESS	
National Aeronautics and Space Administration Washington, D. C. 20546	Technical Memorandum
	14. SPONSORING AGENCY CODE

15. SUPPLEMENTARY NOTES

Prepared by Systems Dynamics Laboratory, Science and Engineering

16. ABSTRACT

An angular momentum management scheme applicable to the Orbiter/Spacelab is described. The basis of the scheme is to periodically maneuver the vehicle through a small angle thereby using the gravity gradient torque to dump momentum from the control moment gyro (CMG) control system. The Orbiter is operated with its principal vehicle axis perpendicular to the orbital plane (POP). Numerous case runs have been conducted on the hybrid simulation and representative cases are included.

17. KEY WORDS	18. DISTRIBUTION STATEMENT
	Unclassified-unlimited Jerry W. Cox

19. SECURITY CLASSIF. (of this report)	20. SECURITY CLASSIF. (of this page)	21. NO. OF PAGES	22. PRICE
Unclassified	Unclassified	60	NTIS

TABLE OF CONTENTS

LIST OF ILLUSTRATIONS

LIST OF ILLUSTRATIONS (Concluded)

DEFINITION OF SYMBOLS

CMG	control moment gyro
H	instantaneous momentum state of the CMG system
H_{AV}	average momentum over the orbital period
H_C	momentum command, reference momentum value of the CMG system at the end of the orbital dumping period
H_{DC}	momentum dump command
H_{SEC}	change in average momentum per orbit
H_ϵ	momentum error, the difference between the instantaneous and command momentum at the end of the orbital dumping period
$I_{\Delta 1}$	$I_2 - I_3$
$I_{\Delta 2}$	$I_3 - I_1$
$I_{\Delta 3}$	$I_1 - I_2$
IOP	in the orbit plane (principal axis)
i	POP orientation label
j	command label in the principal vehicle frame
K	coefficient matrix
K_{PD}	percentage dumping constant indicating the amount of momentum to be removed from the CMG system
LBNP	lower body negative pressure torque (taken from Skylab)
LOS	line-of-sight
MIB	minimum impulse bit (lb-sec)
N	Nth or present orbit
N-1	(N-1)th or previous orbit

DEFINITION OF SYMBOLS (Concluded)

POP	perpendicular to the orbit plane (principal axis)
T. A. No. 1	trash airlock No. 1 vent (taken from Skylab)
T. A. No. 2	trash airlock No. 2 vent (taken from Skylab)
T_o	orbital period
T_s	torque occurrence time (sec)
T_{XBD}	constant biased disturbance torque about X-axis
T_{YBD}	constant biased disturbance torque about Y-axis
T_{ZBD}	constant biased disturbance torque about Z-axis
ϵ	small angular rotation about the vehicle axis, maneuver angle
ϵ_c	commanded attitude of the vehicle relative to the reference frame
ϵ_o	apparent zero momentum accumulation attitude of the vehicle relative to the reference frame
θ	orbital angle
$C\theta$	cos θ
$S\theta$	sin θ
ω_o	orbital rate

TECHNICAL MEMORANDUM X-64873

ORBITER/SPACELAB MOMENTUM MANAGEMENT FOR POP ORIENTATIONS

SUMMARY

This document describes an on-orbit momentum management scheme using small maneuvers while at the same time providing continuous celestial target observation. The basis of the scheme is to periodically maneuver the vehicle through a small angle thereby using the gravity gradient torque to dump momentum from the control moment gyro (CMG) control system. The CMG momentum dumping scheme is applied to the Shuttle Orbiter/Spacelab which could operate in the X-POP, Y-POP, and Z-POP orientations shown in Figure 1. These three orientations and their complement in combination with a double-gimbal telescope will provide complete celestial sphere line-of-sight (LOS) coverage. The scheme involves performing once per orbit a three-axis maneuver soon after momentum error determination, followed by a single axis maneuver on the axis perpendicular to the orbit plane (POP) approximately one-fourth orbit later.

A general discussion of the momentum dumping scheme is presented in Section II. Some typical simulation results are shown in Section III, and conclusions are discussed in Section IV.

I. INTRODUCTION

The Spacelab experiments require an attitude to provide continuous celestial target observation. To attain complete celestial sphere LOS coverage, the Shuttle Orbiter is held in an inertial orientation. Using both a coarse and fine gimbal system, a target can be observed. Use of two of the POP orientations in combination with the telescope gimbal control angles will provide complete celestial sphere LOS coverage as shown in Figure 2.

Gravity gradient, aerodynamic, and other torques acting on the vehicle while performing these experiments must be stored by a momentum storage device, and for Spacelab, a system of three double-gimbal CMG's could be used. Noncyclic torques exist and tend to saturate the CMG system, which is

limited in its storage capacity. To avoid saturation of the CMG system, momentum is removed (dumped) by periodically maneuvering the vehicle to a slightly different attitude, thus allowing the gravity gradient torque to dump momentum from the CMG control system.

II. MOMENTUM MANAGEMENT SCHEME MODEL

Because of its orbital altitudes, the Spacelab will primarily be affected by disturbances resulting from the gravitational field of the earth. The gravity gradient torque acting on the vehicle can be expressed as

$$\bar{T}_{GG} = 3\omega_o^2 \, \tilde{r} I \bar{r} \quad , \tag{1}$$

when the vehicle is in a circular orbit. ω_o is the orbital rate ($\omega_o = \sqrt{M/R^3}$), I is the vehicle inertia matrix, $\bar{r}$ is a unit vector directed along the radius vector from center of the earth to the vehicle center of mass, and $\tilde{r}$ is defined as

$$\tilde{r} = \begin{bmatrix} 0 & -r_3 & r_2 \\ r_3 & 0 & -r_1 \\ -r_2 & r_1 & 0 \end{bmatrix} \quad . \tag{2}$$

In matrix form, when the vehicle axes are principal axes of inertia, the gravity gradient torque becomes

$$\begin{Bmatrix} T_{GG_1} \\ T_{GG_2} \\ T_{GG_3} \end{Bmatrix} = 3\omega_o^2 \begin{Bmatrix} (I_3 - I_2) & r_2 & r_3 \\ (I_1 - I_3) & r_3 & r_1 \\ (I_2 - I_1) & r_1 & r_2 \end{Bmatrix} \quad . \tag{3}$$

The gravity gradient torque and therefore the angular momentum accumulated by the CMG's of a vehicle in an inertial orientation depend on the vehicle's orientation relative to the earth's local vertical; i.e., the direction cosines r_1, r_2, and r_3 of equation (3).

When the vehicle's principal axis is perpendicular to the orbit plane, the gravity gradient torque consists of a nonbias cyclic component on the vehicle POP axis having a period equal to half that of the orbit and zero components on the vehicle in-plane axis. Since momentum is the integral of the torque, no momentum will be accumulated because of the gravity gradient torque. If, however, the vehicle has an angular displacement from the POP orientation, the torque components on the vehicle POP axis will remain a nonbias cyclic function. The torque component on each of the vehicle's in-plane axis will have a bias torque causing the vehicle to accumulate momentum.

A momentum management (dump) scheme using small maneuvers which would be suitable for Spacelab operating in a POP orientation was developed.[1] To dump the accumulated momentum of the in-plane axis, a small rotation about the in-plane axis will change the bias component of the gravity gradient torque which can be used as a control torque to dump accumulated momentum from the CMG's. The average torque capability available per orbit for momentum dumping can be expressed as

$$T_{GD_{ij}} = \hat{T}_{GG_{ij}} = \frac{1}{T_o} \int_0^{T_o} T_{GG_{ij}} \, dt \quad , \tag{4}$$

where

$T_{GD_{ij}}$ is the gravity gradient dump torque capability

i is the POP orientation label

j is the component label in the principal vehicle frame

T_o is the orbital period.

1. Howell, J. T.: Momentum Dumping Scheme for Shuttle/Sortie Lab. S&E-AERO-DO-41-73, September 18, 1973.

A summary of the momentum dumping capability (H_D) per orbit for a vehicle inertially held is then calculated by

$$H_D = T_{GD_{ij}} T_o = \int_0^{T_o} T_{GG_{ij}} dt \quad . \tag{5}$$

A "pair" of small maneuvers about the vehicle POP axis when properly executed (timed) will result in a bias gravity gradient torque on that axis which can be used as a control torque to dump accumulated momentum from the same axis of the CMG control system. A "pair" of properly timed maneuvers effects a bias torque by altering the shape of the gravity gradient torque profile from the symmetric sinusoid, characteristic of a vehicle inertially held in a POP orientation.

In the dump scheme simulation, the paired maneuver used was the position/position maneuver illustrated in Figure 3. The position/position maneuver is an idealistic maneuver in that an infinite vehicle maneuver rate is assumed that provides an instantaneous change in vehicle orientation. This simplification provides an overview of the mechanism of the proposed momentum dumping scheme. In addition, for a reasonable vehicle maneuver rate such as that equal to half the orbital rate, a small angle maneuver can be accomplished in several minutes, which is a small percentage of the total orbital period.

Figure 3 illustrates how the gravity gradient torque profile is altered for the position/position maneuver. At time t_1, the vehicle is rotated through a small angle about the vehicle POP axis which introduces a phase shift of the gravity gradient torque profile. One-fourth orbit later ($t_2 = t_1 + T_{o/4}$), the vehicle is rotated through the negative of the first rotation, thus returning the vehicle to its original inertial orientation and torque profile.

In Figure 3(a) the first rotation at t_1 (just past the peak of a positive lobe) has the same sense as the orbital angular velocity vector (ω_o). This will effect an increase in the area under the positive lobe of the torque curve and consequently provide a positive increase in momentum to be accumulated. A rotation of opposite sense at t_2 (prior to the peak of the negative lobe) reduces the area under the negative lobe providing an additional and equal increase in momentum.

In Figure 3(b) the vehicle is first rotated at t_1, in the opposite sense as the orbital angular velocity vector (ω_o) and then in the same sense at t_2. For this case, there is a decrease of positive area and an increase of negative area, both resulting in a decrease of momentum accumulated.

The momentum dumping scheme described above and the corresponding equations are presented in detail in the Appendix.

III. TYPICAL SIMULATION RESULTS

The momentum desaturation method for the Shuttle Orbiter/Spacelab configuration utilizing the gravity gradient torques has been simulated. The scheme consists first of making a small rotation about the in-plane axes once per orbit, then making a pair of small properly timed rotations about the POP axis each orbit.

Numerous case runs have been conducted on the 8900 hybrid simulation. All simulations were made using a run speed of 100 times real time and a 370-km (200-n. mi.) orbit with an inclination angle of 55 deg. Graphical results of some of these studies are shown in Figures 4 through 28 where

PHIXC — commanded maneuver angle about vehicle X-axis

PHIYC — commanded maneuver angle about vehicle Y-axis

PHIZC — commanded maneuver angle about vehicle Z-axis

HXCMG — CMG total momentum about vehicle X-axis

HYCMG — CMG total momentum about vehicle Y-axis

HZCMG — CMG total momentum about vehicle Z-axis

HMCMG — total CMG momentum magnitude

ETAT — vehicle angular position in orbit measured from orbital midnight.

Figures 4 through 12 show cases for initial rates being applied to the vehicle. This analysis considered the transfer of control from the 950-lb reaction control system (RCS) thrust level operating in a minimum impulse bit (MIB) mode to a CMG control mode. Maximum residual rates were determined

and assigned as initial rates as CMG control was initiated. The largest rates were those for MIB = 33 lb-sec which were 0.0299 deg/sec in roll, 0.0369 deg/sec in pitch, and 0.0179 deg/sec in yaw.

Figures 4 through 6 are for X-POP orientations. The initial rates for case 4 were 5 percent of the largest rates and for case 5 were 10 percent of the largest rates. The transfer of angular rates by the change of control modes also causes a transfer of angular momentum. The amount of momentum transferred increases as the angular rates increase. To control this increase in momentum, a larger maneuver angle is commanded by the dump scheme. This can be seen in Figure 6 where the commanded roll angle is on the 10-deg assigned limit.

Figures 7 through 9 are for Y-POP orientations, and Figures 10 through 12 are for Z-POP orientations. For these cases, the largest commanded maneuver angle is 1.6 deg which is for Z-POP orientation with MIB = 3 lb-sec.

Figures 13 through 21 illustrate results of aerodynamic disturbances and a constant biased disturbance torque (T_{XBD}, T_{YBD}, T_{ZBD}) being applied to the vehicle. Figure 13 shows an X-POP orientation with a biased disturbance torque about the POP axis of 0.03 N-m. This torque was the largest permissible in order to keep the commanded maneuver angle below the 10-deg assigned limit. Figures 14 and 15 show for X-POP a constant torque about the Y-axis and Z-axis respectively. Here, the largest torque applied was 1 N-m.

Figures 16 through 18 illustrate the effects of a biased torque for the Y-POP orientations. Figure 17 shows the largest permissible torque about the POP axis of 0.8 N-m in order to keep the commanded maneuver angle below the 10-deg assigned limit.

Figures 19 through 21 show the effects of a constant biased torque for the Z-POP orientations. Figure 21 illustrates the largest permissible torque about the POP axis of 0.8 N-m which allows the imposed limit of the maneuver angle to be satisfied.

Figures 22 and 23 are for X-POP orientations having torques applied to the vehicle by typical housekeeping vents. The two different vent torques applied were taken from Skylab data and occurred at 14 000 sec (halfway into the third orbit).

Figures 24 through 28 show cases having torques applied to the vehicle by a typical scientific vent. This torque was also obtained from Skylab data. The magnitude of the torque was 0.346 N-m about the X-axis, 3.46 N-m about

the Y-axis, and 2.76 N-m about the Z-axis. Figures 24 through 26 illustrate the effects of the vent torque being applied at 14 000 sec for the X-POP, Y-POP, and Z-POP respectively. Figures 27 and 28 give the results of applying the torques during the first and second orbit respectively for the Z-POP orientation. The commanded maneuver angle for the orbit following the orbit in which the vent torque occurred remained unchanged for the three different event times.

Figures 29 through 31 show the results of having aerodynamic disturbances acting on the vehicle. Several orbital altitudes were studied for the three different POP orientations. The range of commanded maneuver angles for all axes is given by the bars with the steady state angle shown by the darkened area.

IV. CONCLUSIONS

The vehicle disturbance torques are much lower for POP orientations than for previously used X-IOP orientations; thus, less momentum management capability is required. However, the POP orientation scheme will require a coarse telescope control system for "off axis" pointing as well as a fine control system to place the telescope on target.

Simulation showed that the CMG momentum dumping scheme for POP orientations performed very satisfactorily. For the initial rates cases, the assigned limited maneuver angle of 10 deg was reached on one case, that being an X-POP orientation when large initial rates were assigned. However, after three orbits the maneuver angle was reduced considerably.

When constant biased disturbance torques were applied about the POP axis or the X-axis, the limited maneuver angle of 10 deg was reached or nearly reached. In some cases this occurred throughout the run.

The scheme did manage the momentum buildup for all cases involving the torques created by the Skylab type scientific and housekeeping vents.

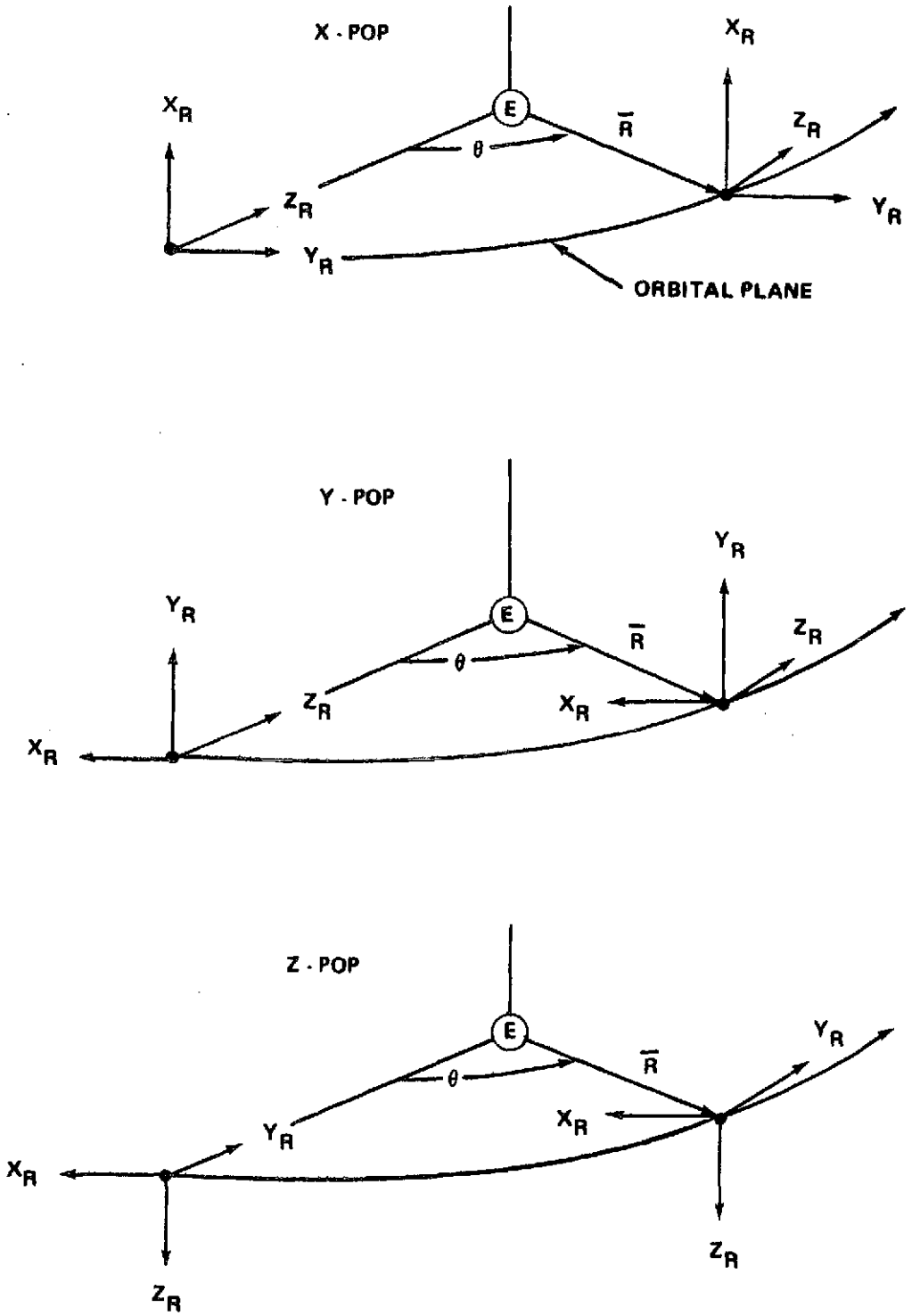

Figure 1. X-POP, Y-POP, and Z-POP reference frames.

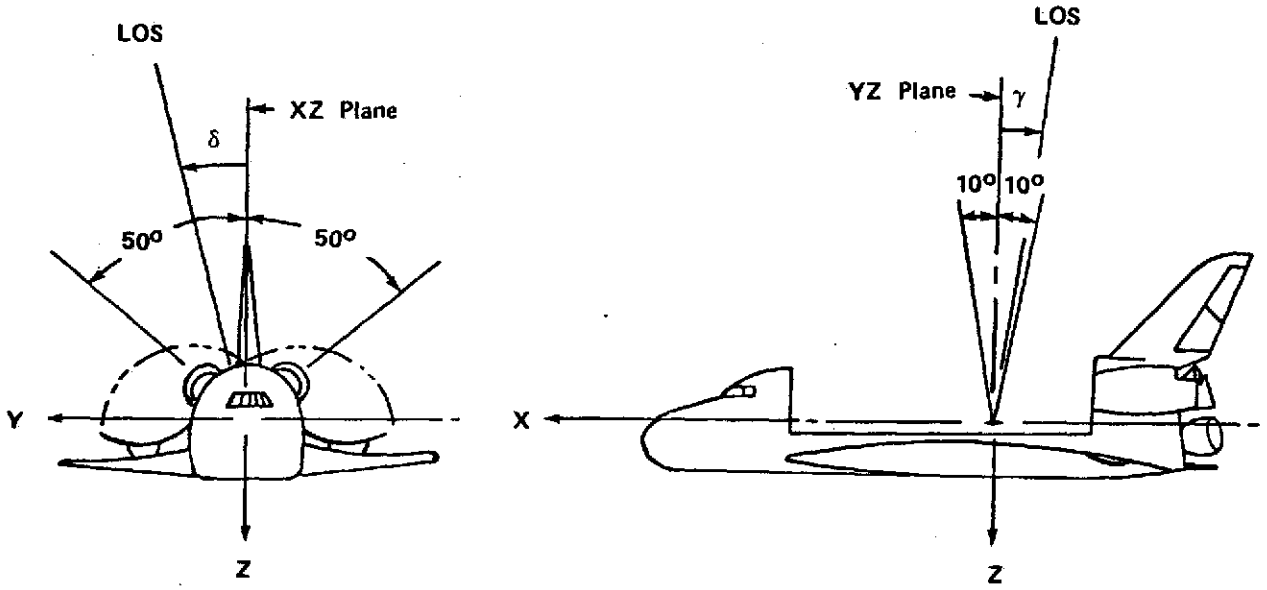

Figure 2. Experiment coarse LOS angles.

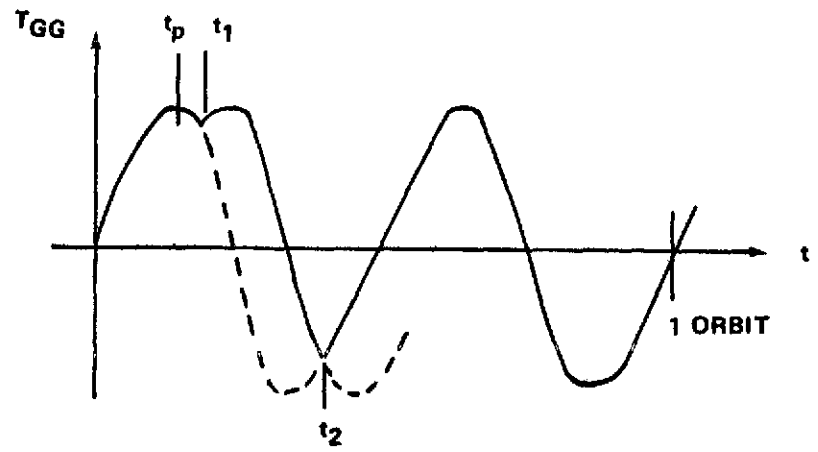

(a) Position/position maneuver.

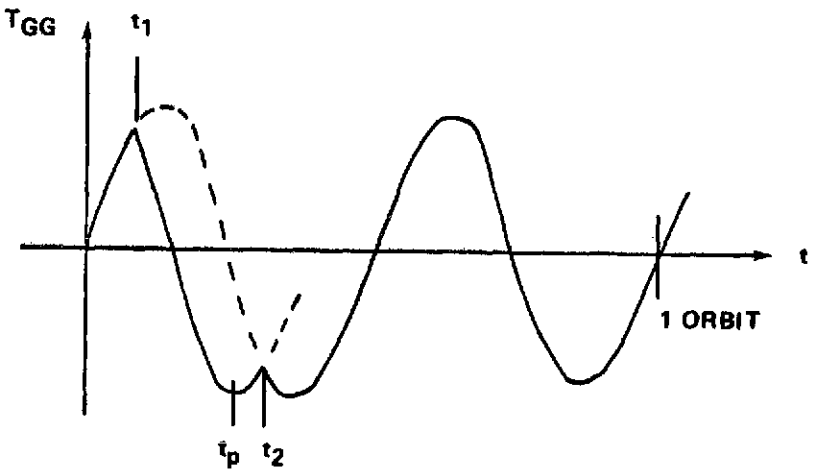

(b) Position/position maneuver.

Figure 3. POP axis gravity gradient profile.

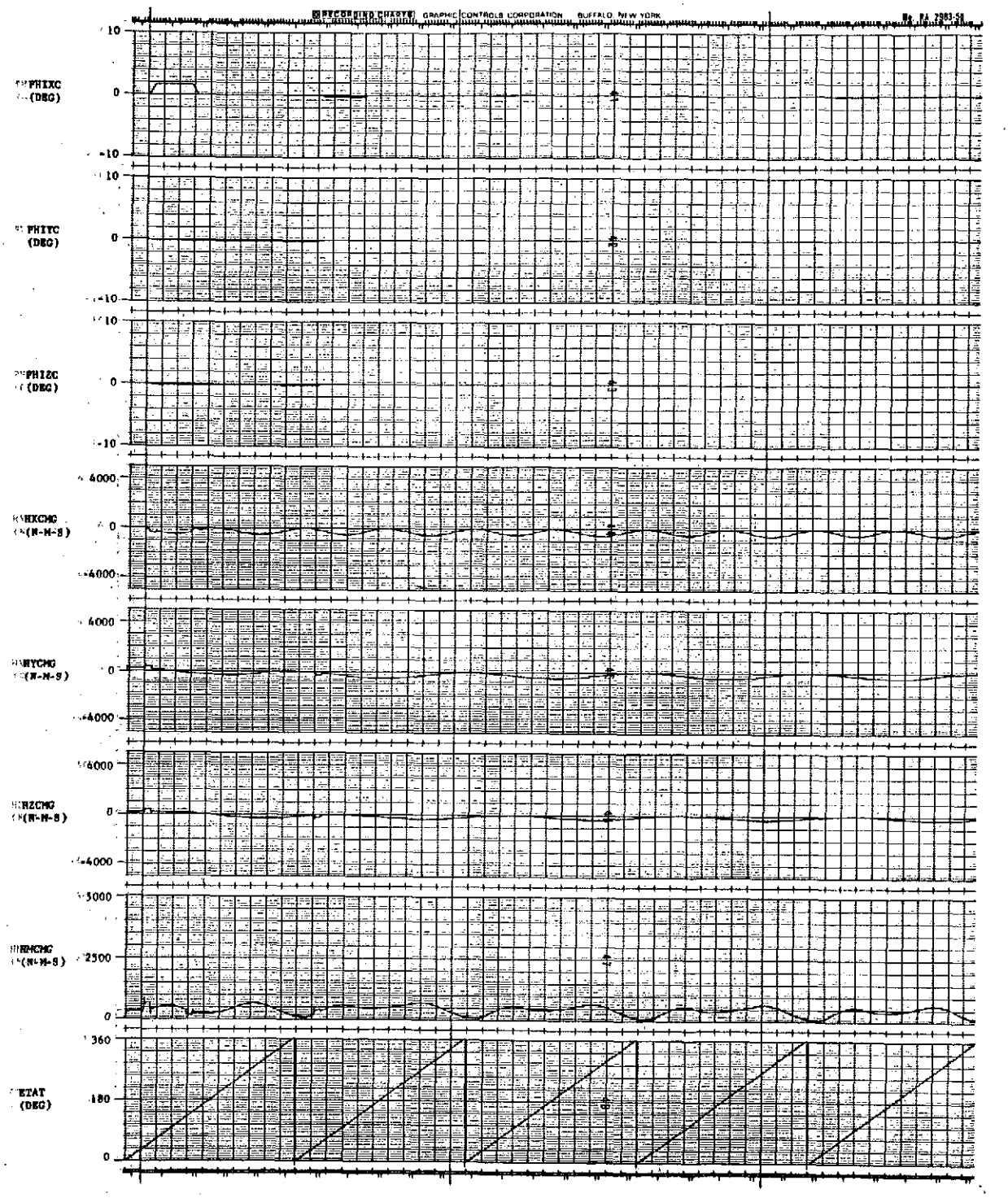

Figure 4. X-POP, initial rates, MIB = 1.5 lb-sec.

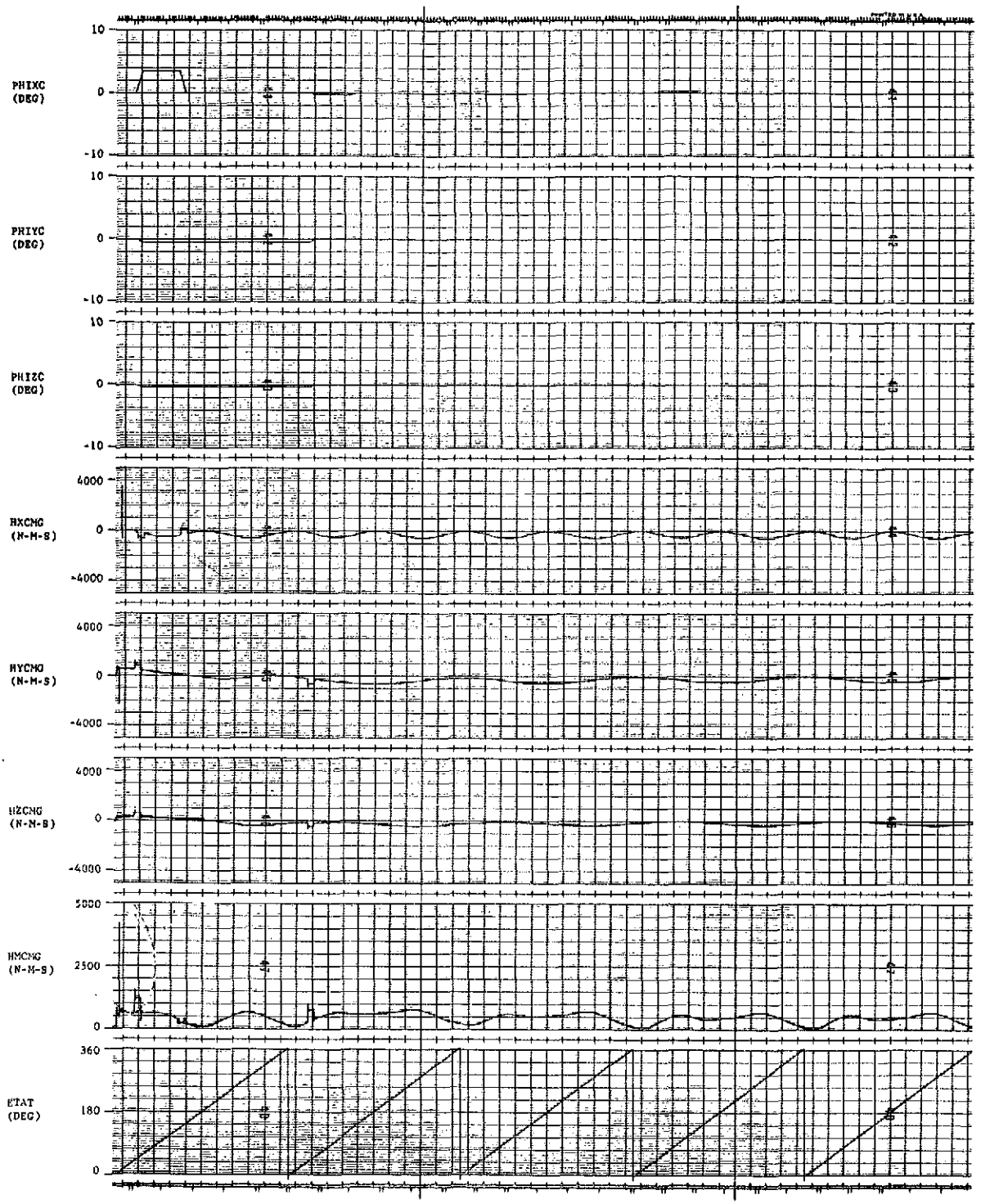

Figure 5. X-POP, initial rates, MIB = 3.0 lb-sec.

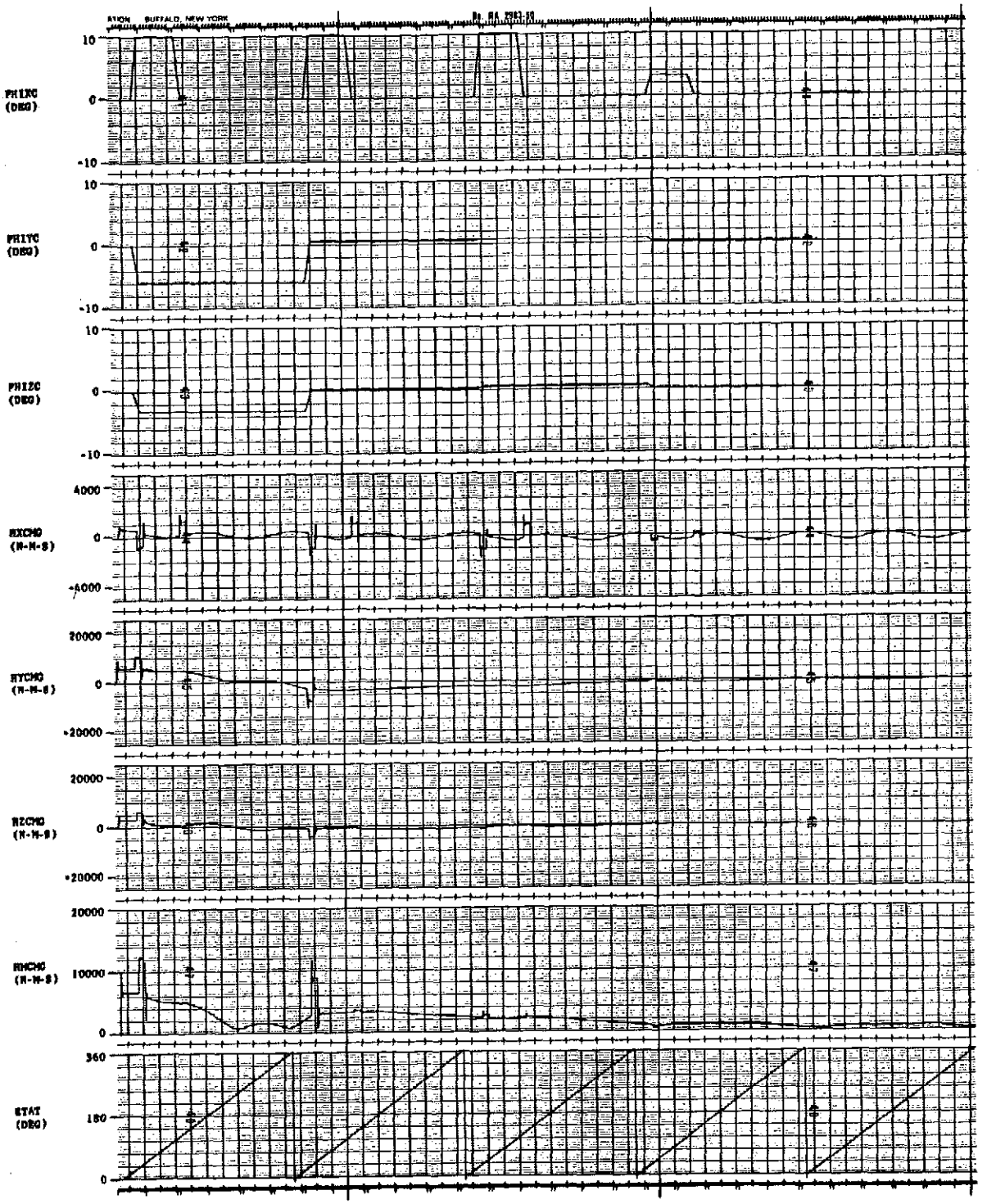

Figure 6. X-POP, initial rates, MIB = 33 lb-sec.

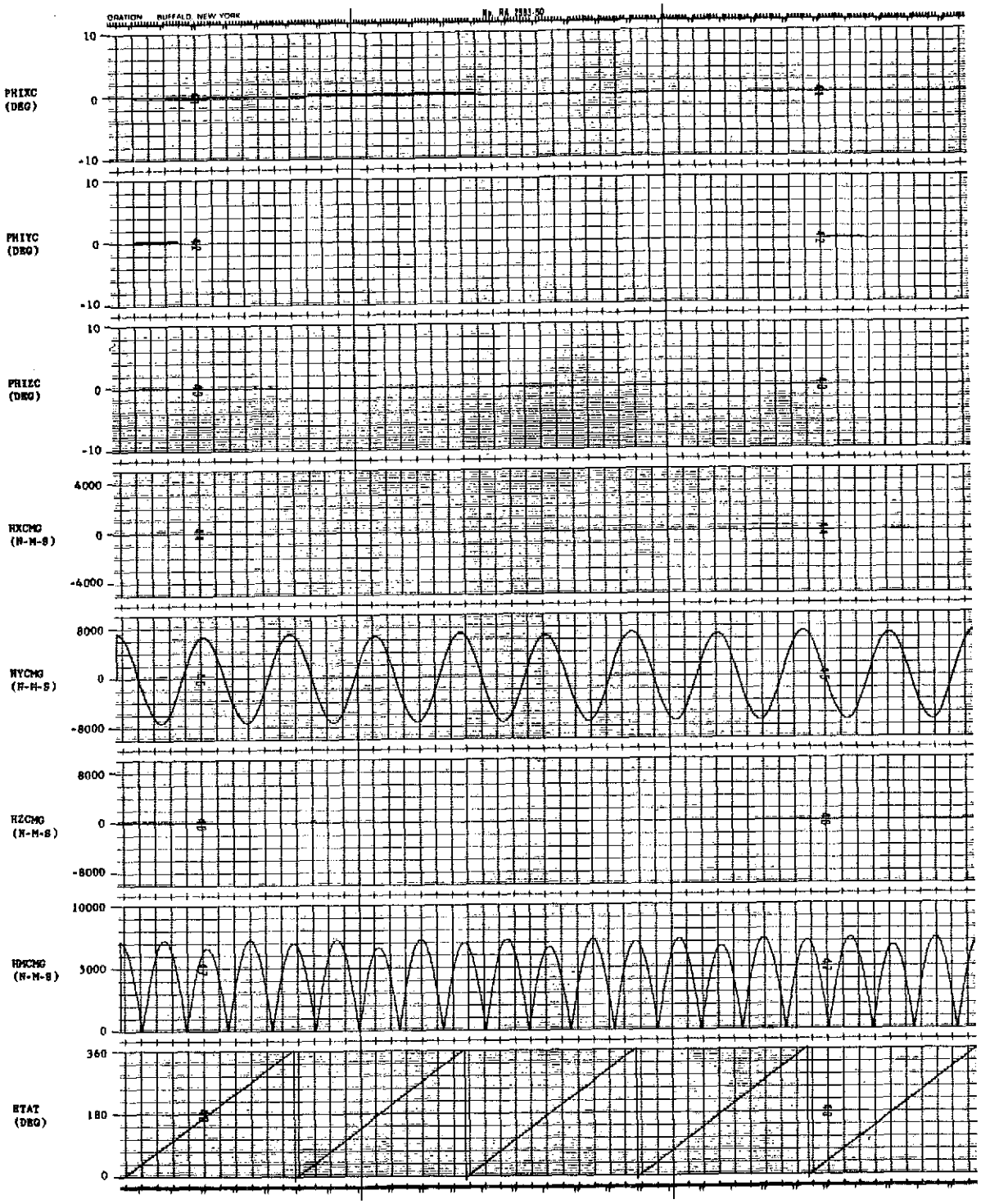

Figure 7. Y-POP, initial rates, MIB = 0.75 lb-sec.

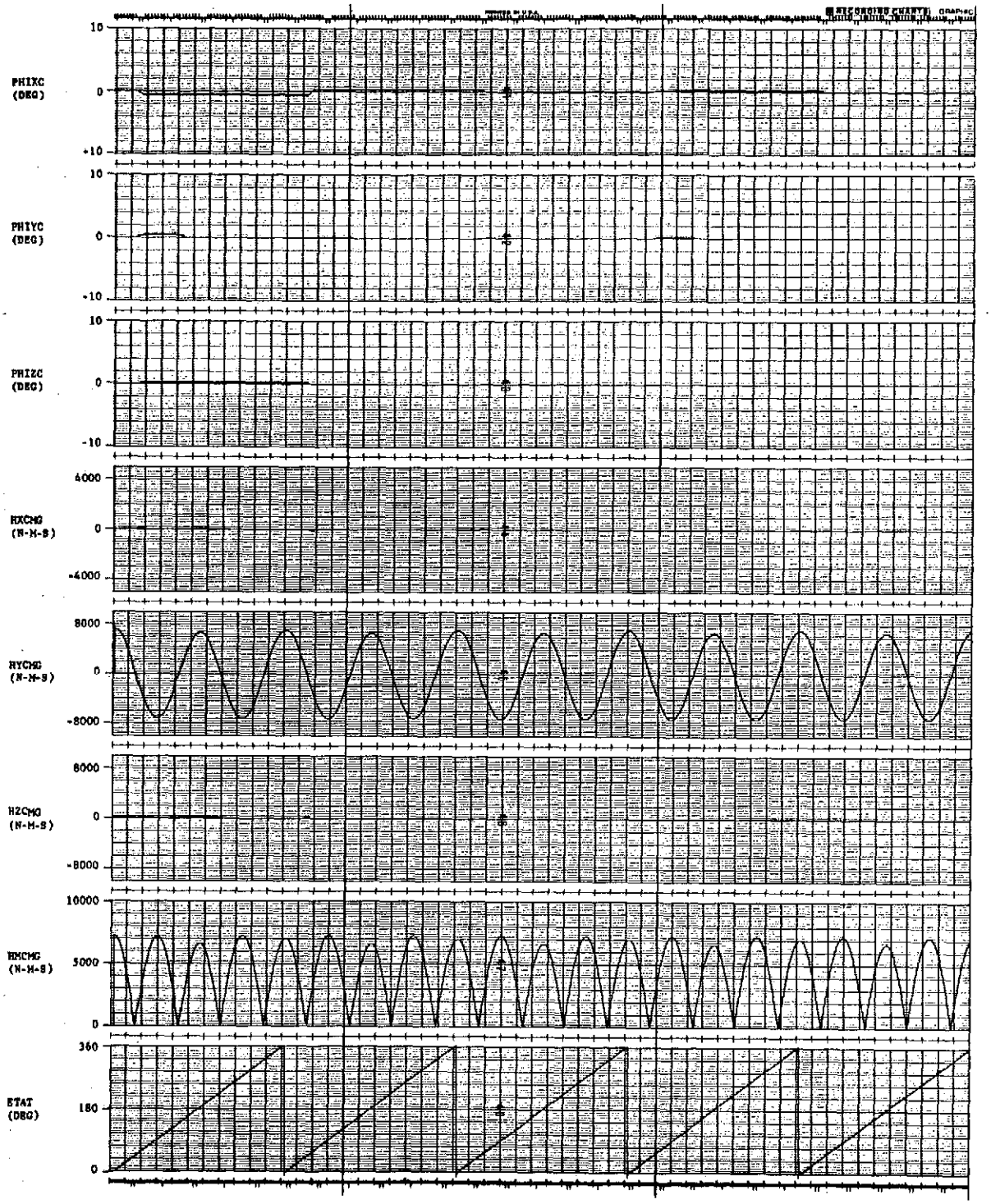

Figure 8. Y-POP, initial rates, MIB = 1.5 lb-sec.

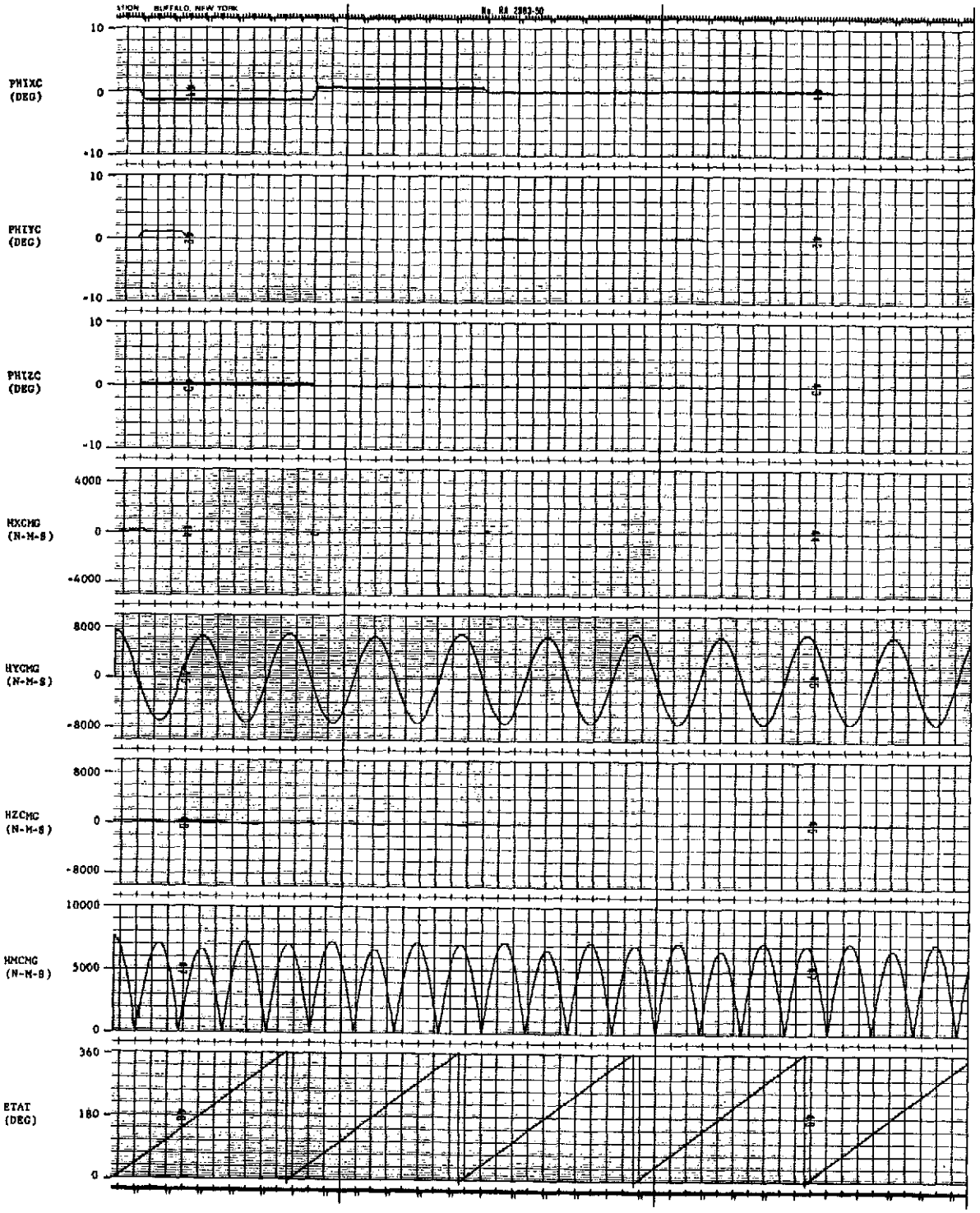

Figure 9. Y-POP, initial rates, MIB = 3.0 lb-sec.

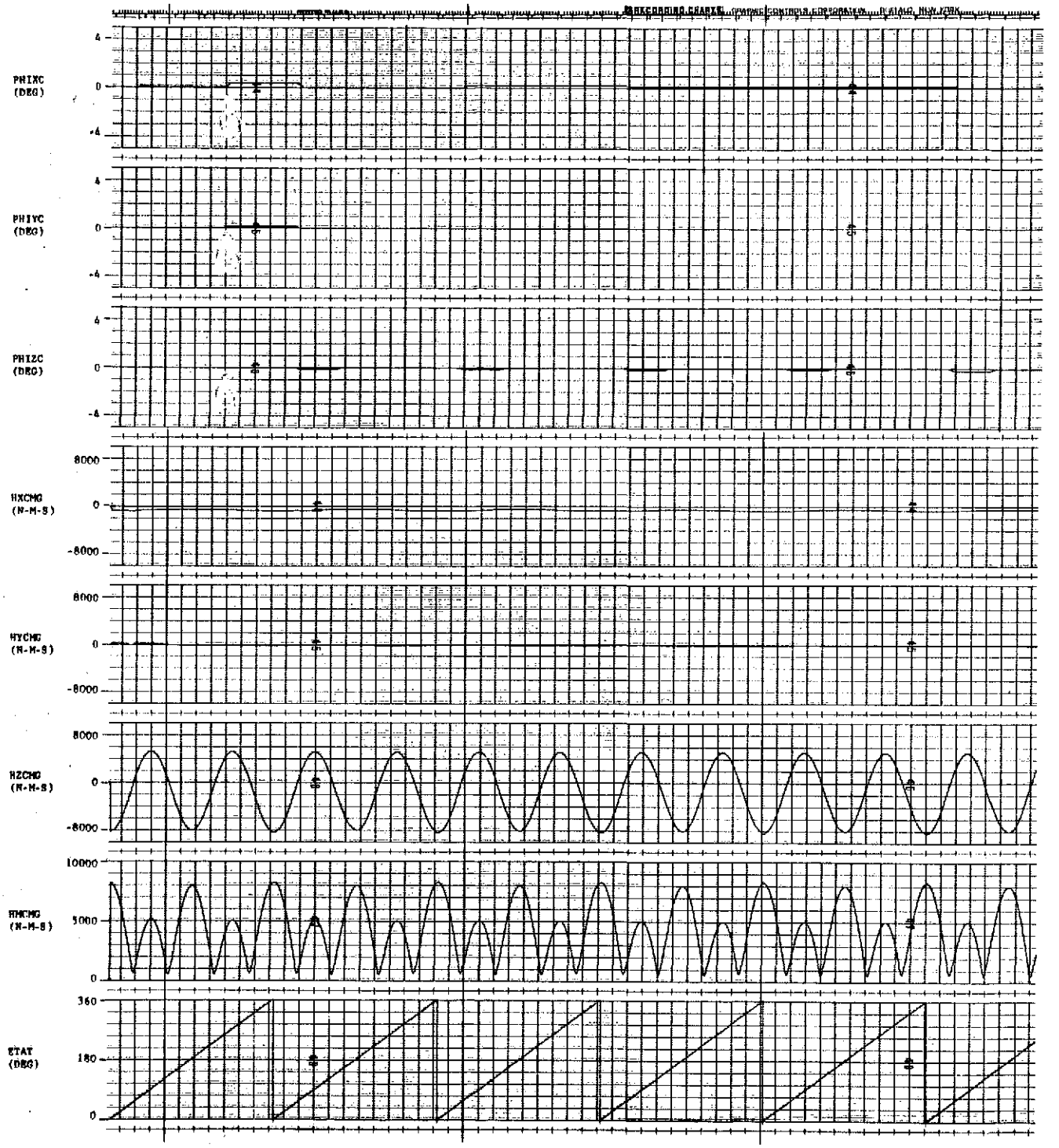

Figure 10. Z-POP, initial rates, MIB = 0.75 lb-sec.

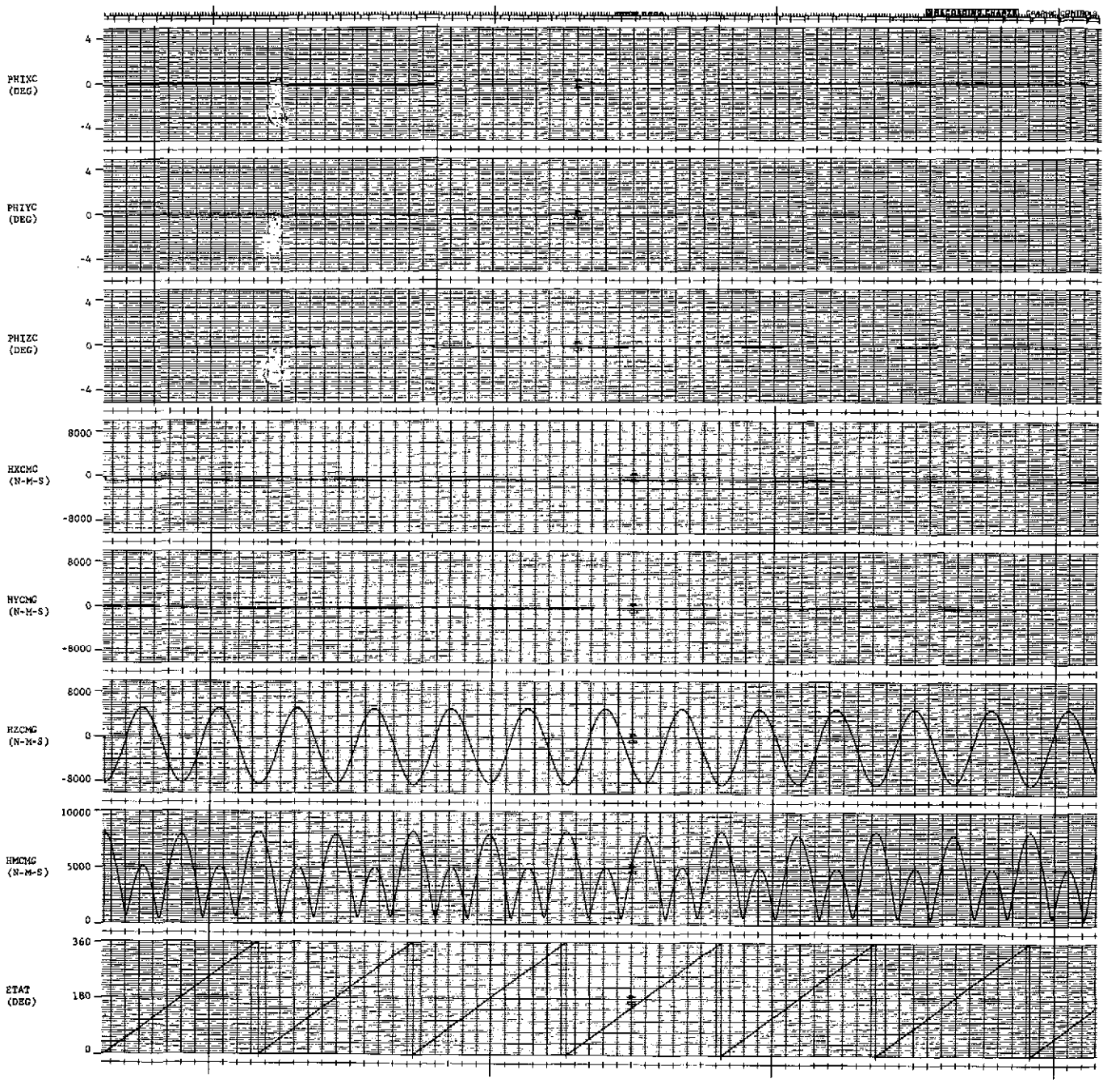

Figure 11. Z-POP, initial rates, MIB = 1.5 lb-sec.

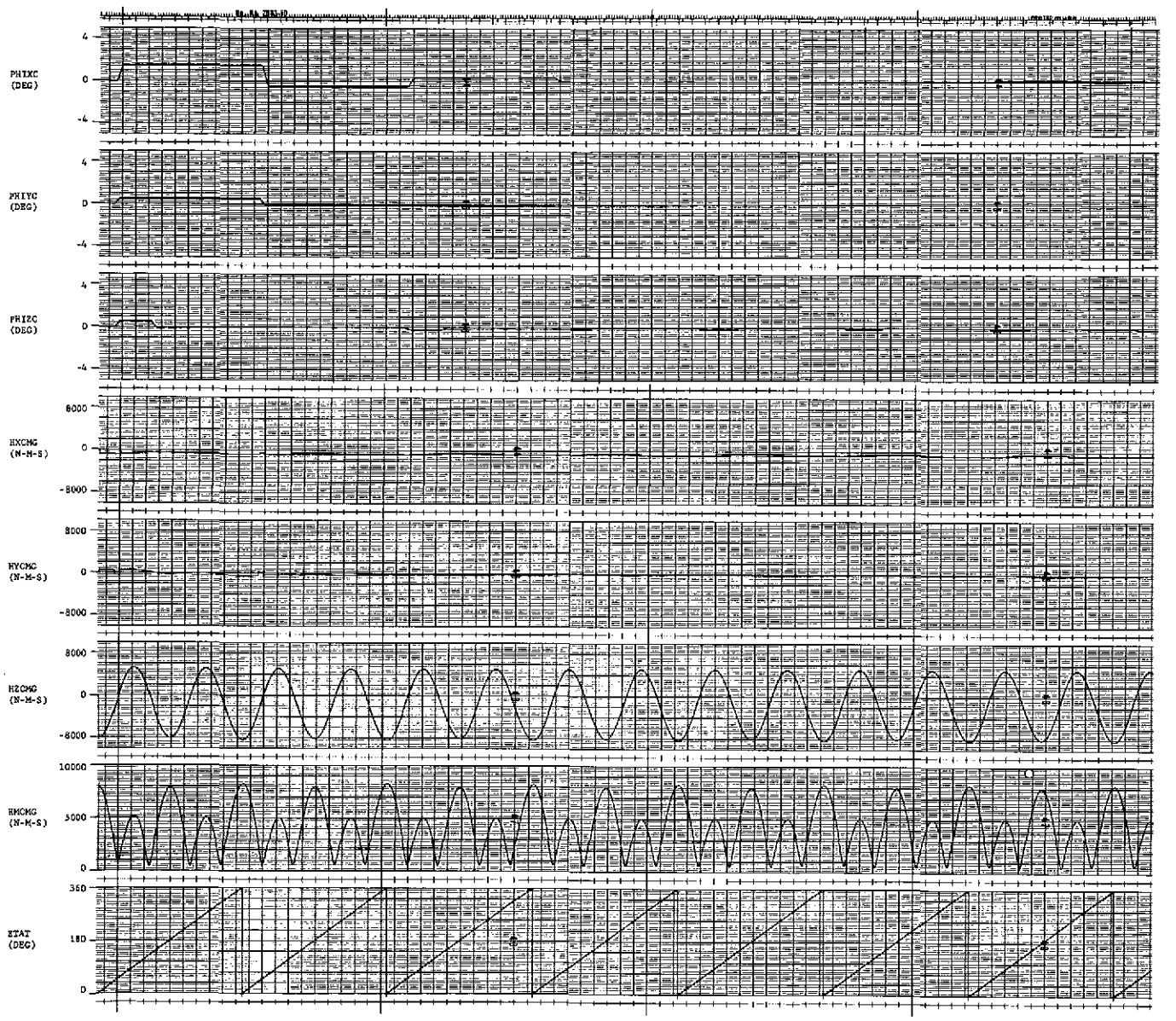

Figure 12. Z-POP, initial rates, MIB = 3.0 lb-sec.

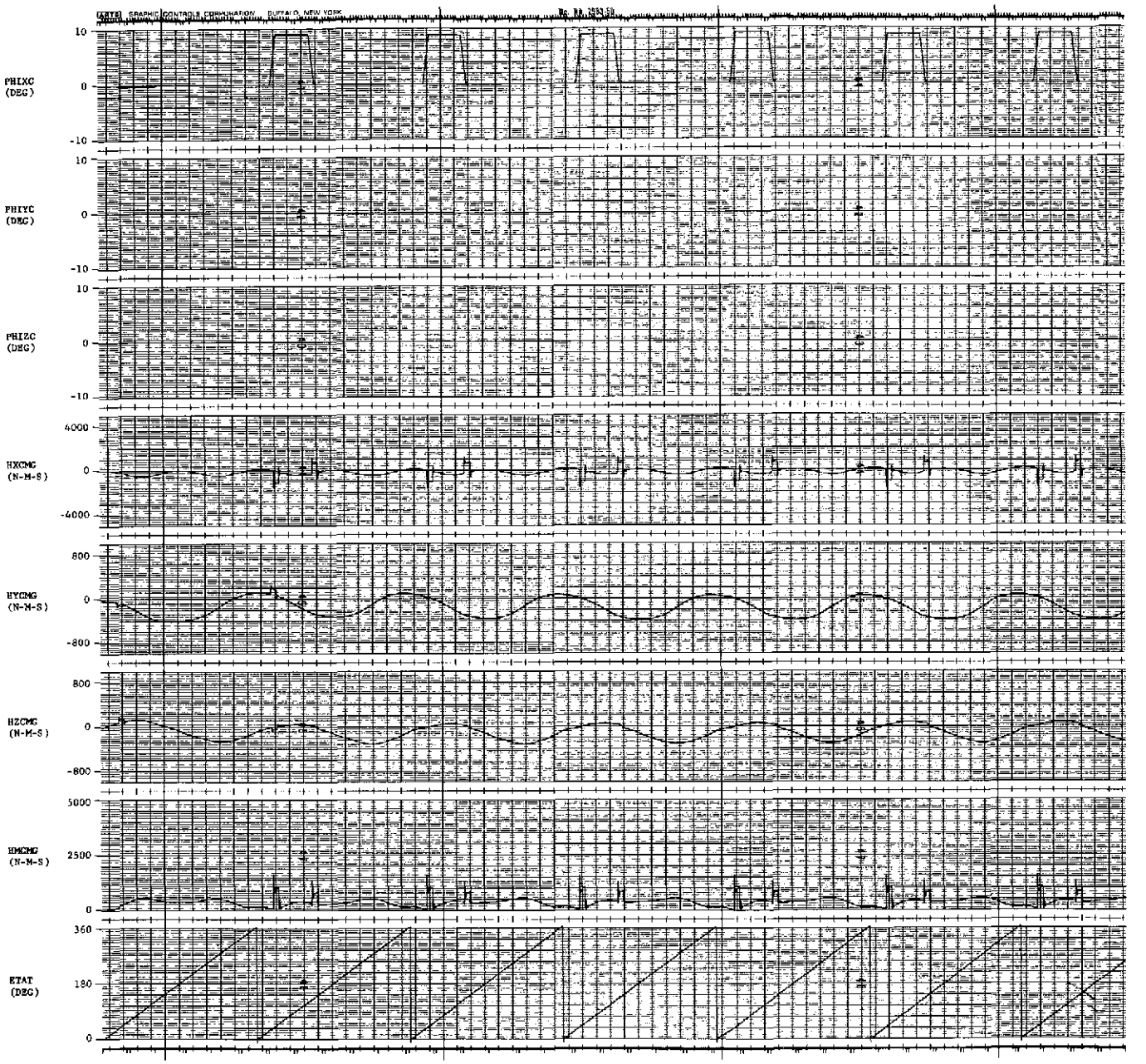

Figure 13. X-POP, $T_{XBD} = 0.03$ N-m.

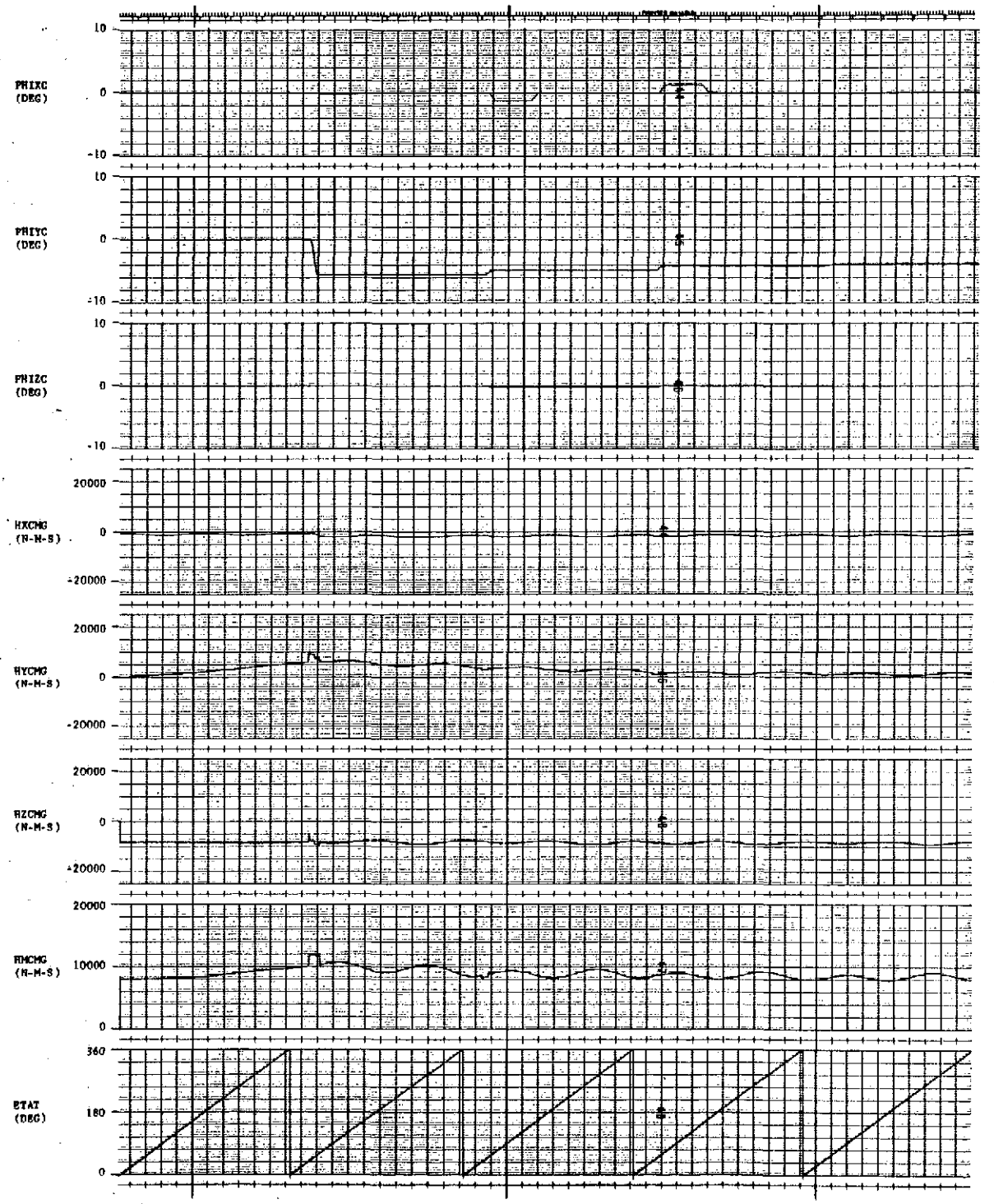

Figure 14. X-POP, T_{YBD} = 1.0 N-m.

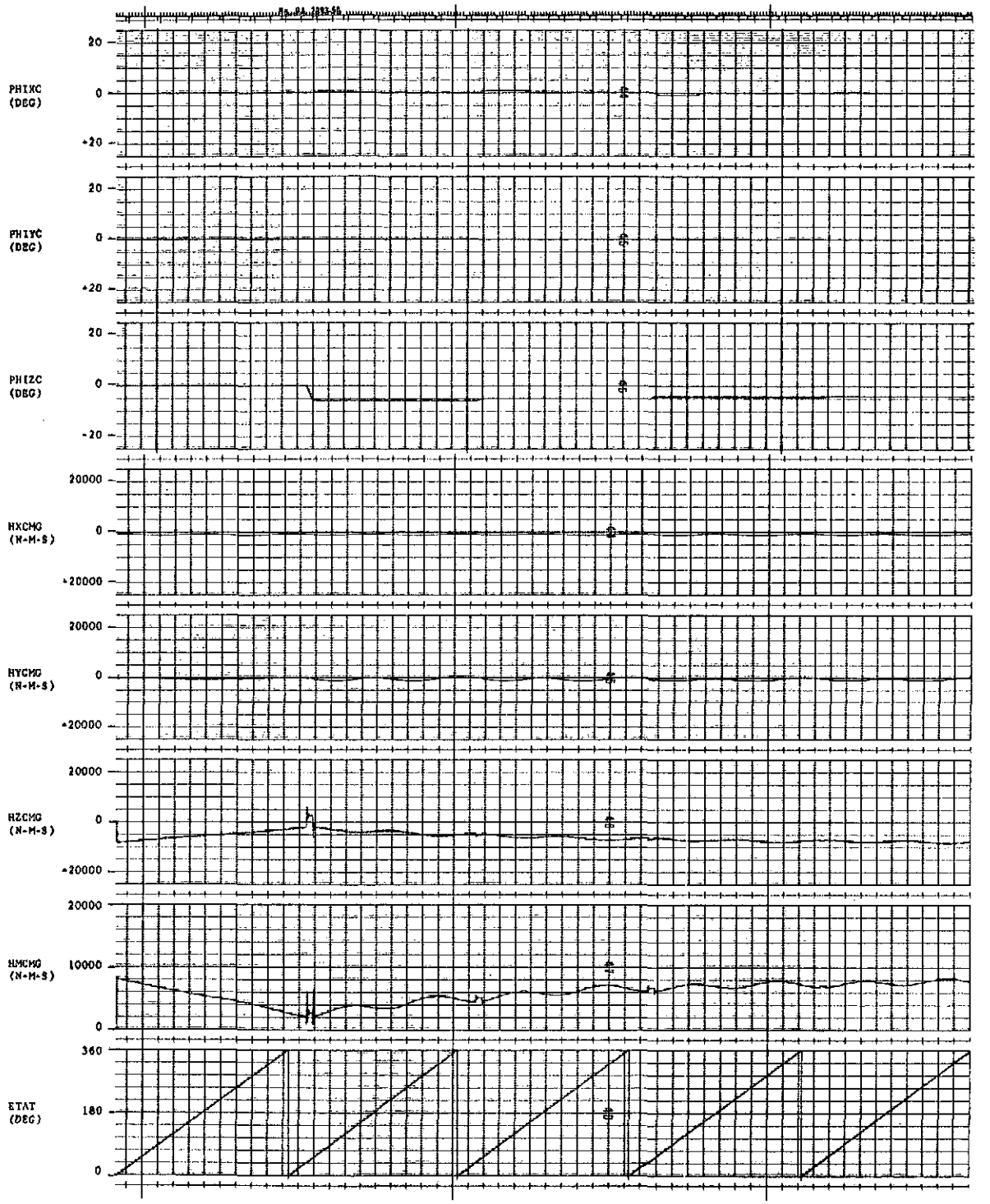

Figure 15. X-POP, T_{ZBD} = 1.0 N-m.

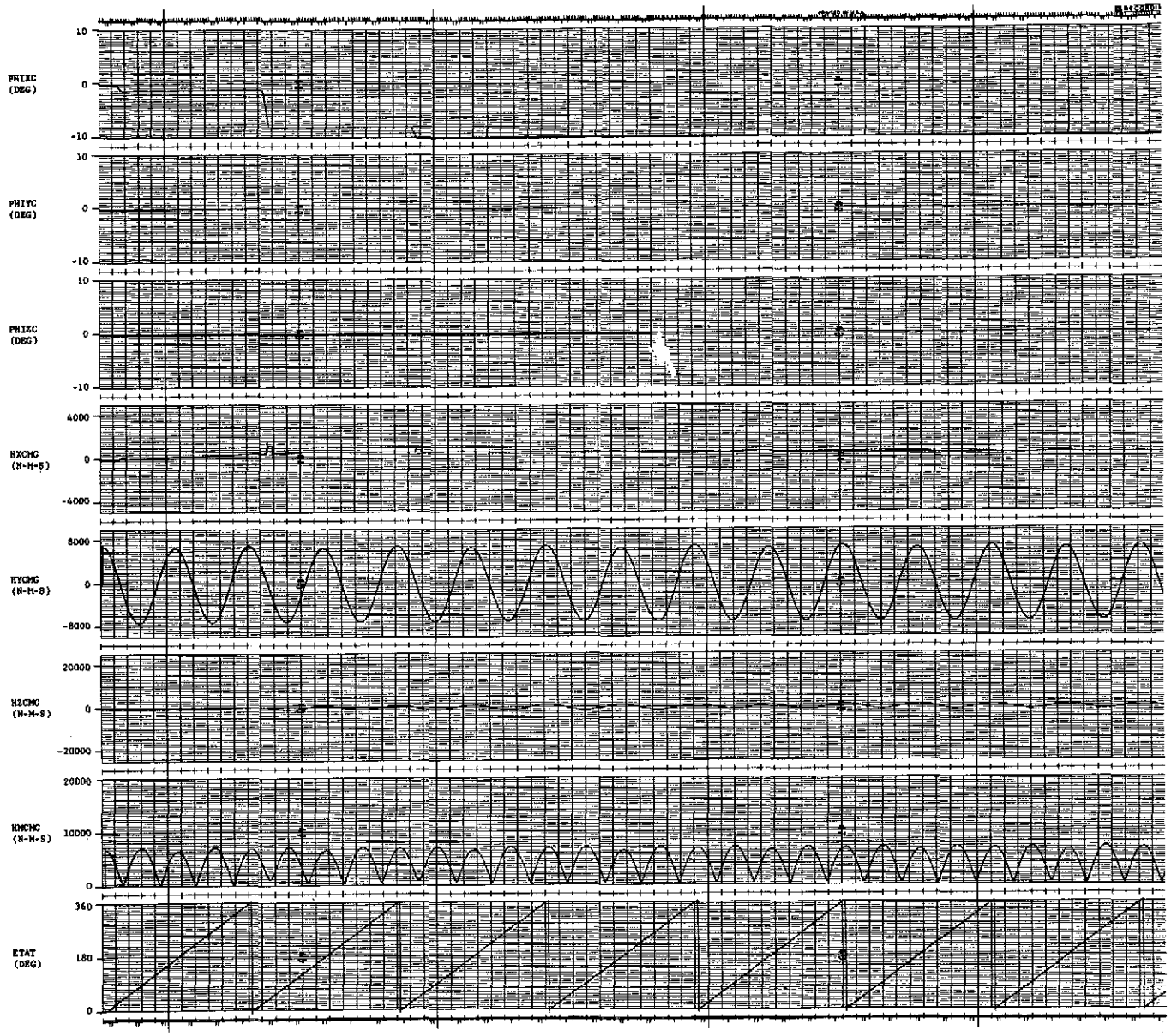

Figure 16. Y-POP, T_{XBD} = 0.1 N-m.

Figure 17. Y-POP, T_{YBD} = 0.8 N-m.

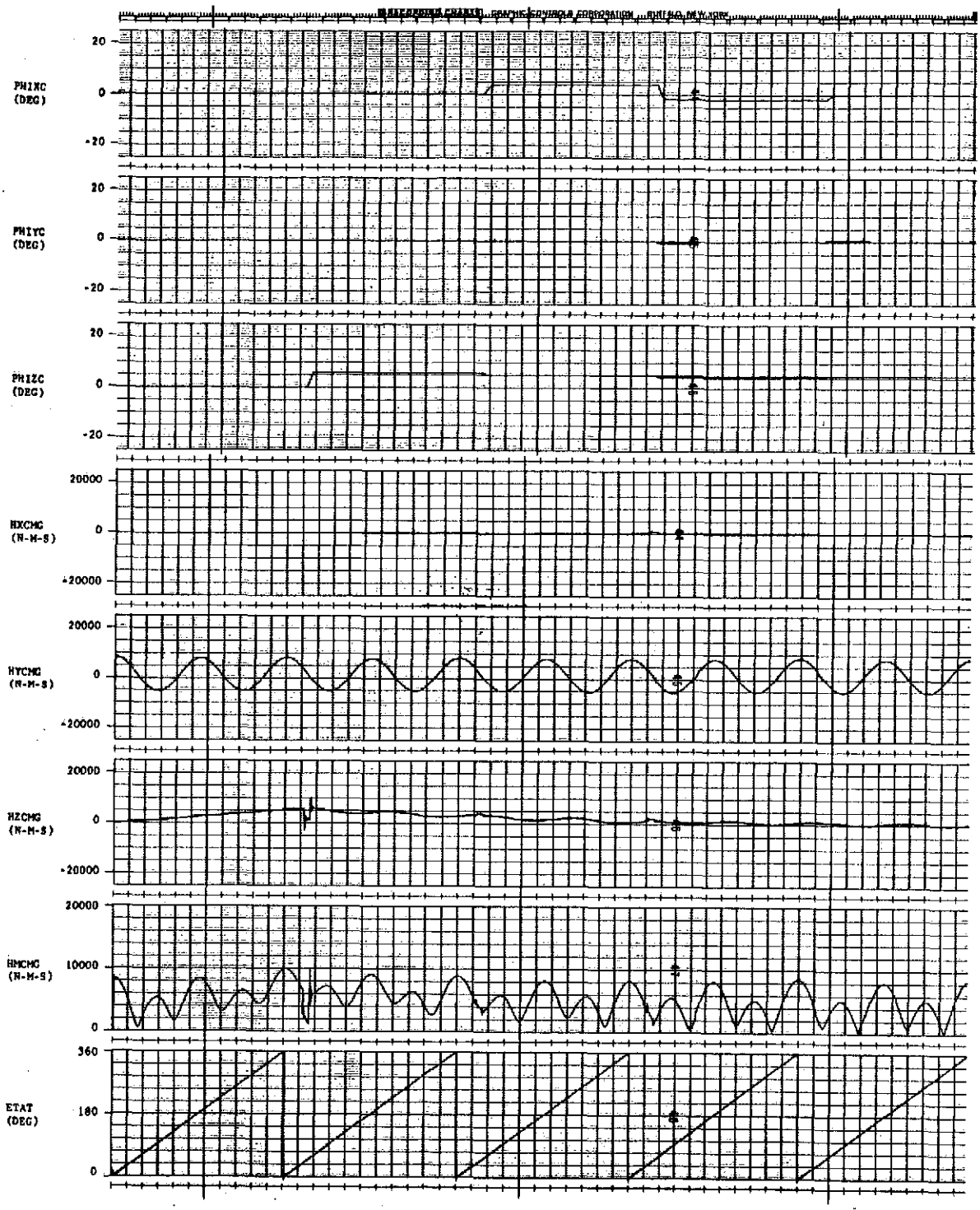

Figure 18. Y-POP, T_{ZBD} = 1.0 N-m.

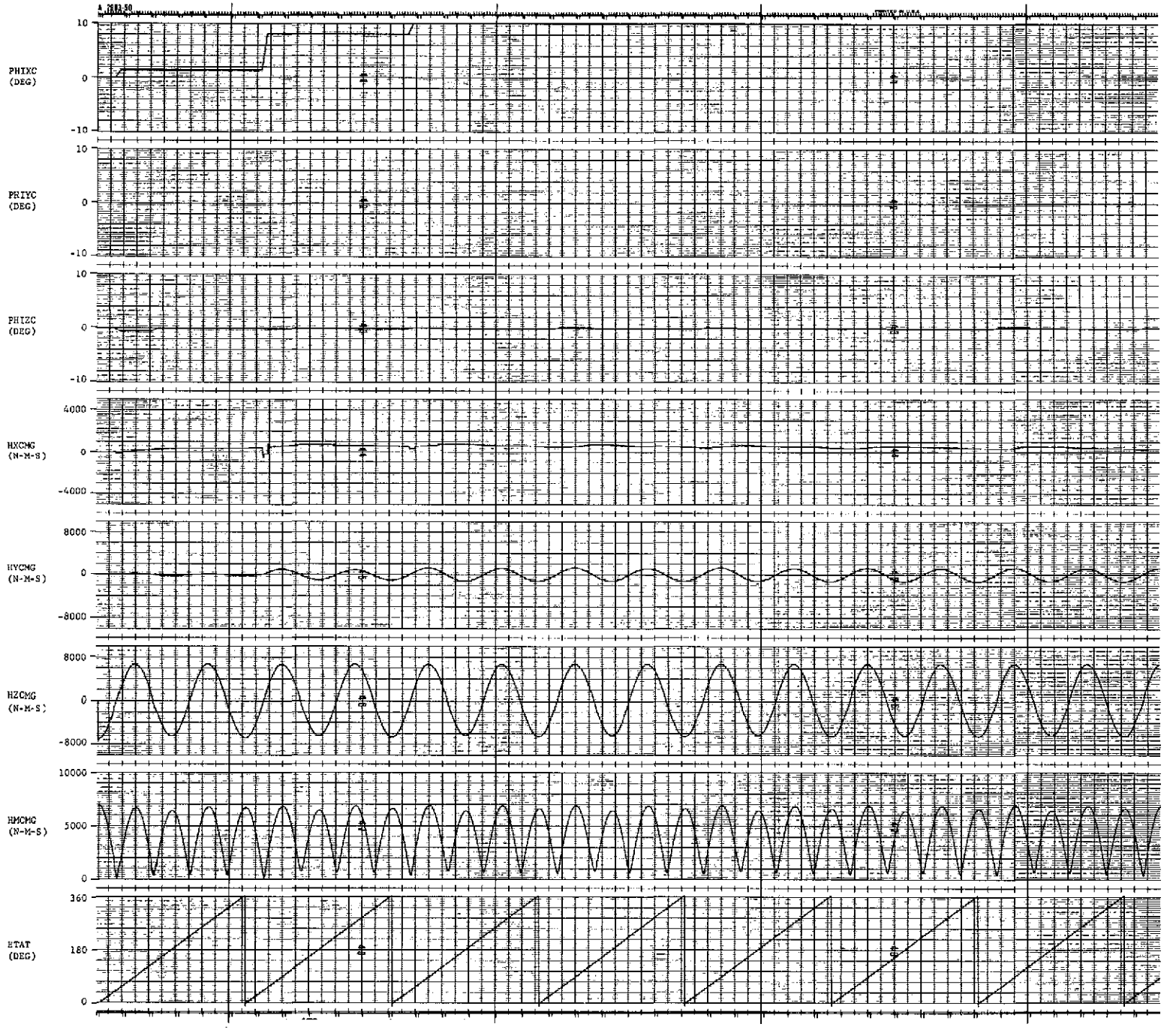

Figure 19. Z-POP, T_{XBD} = 0.1 N-m.

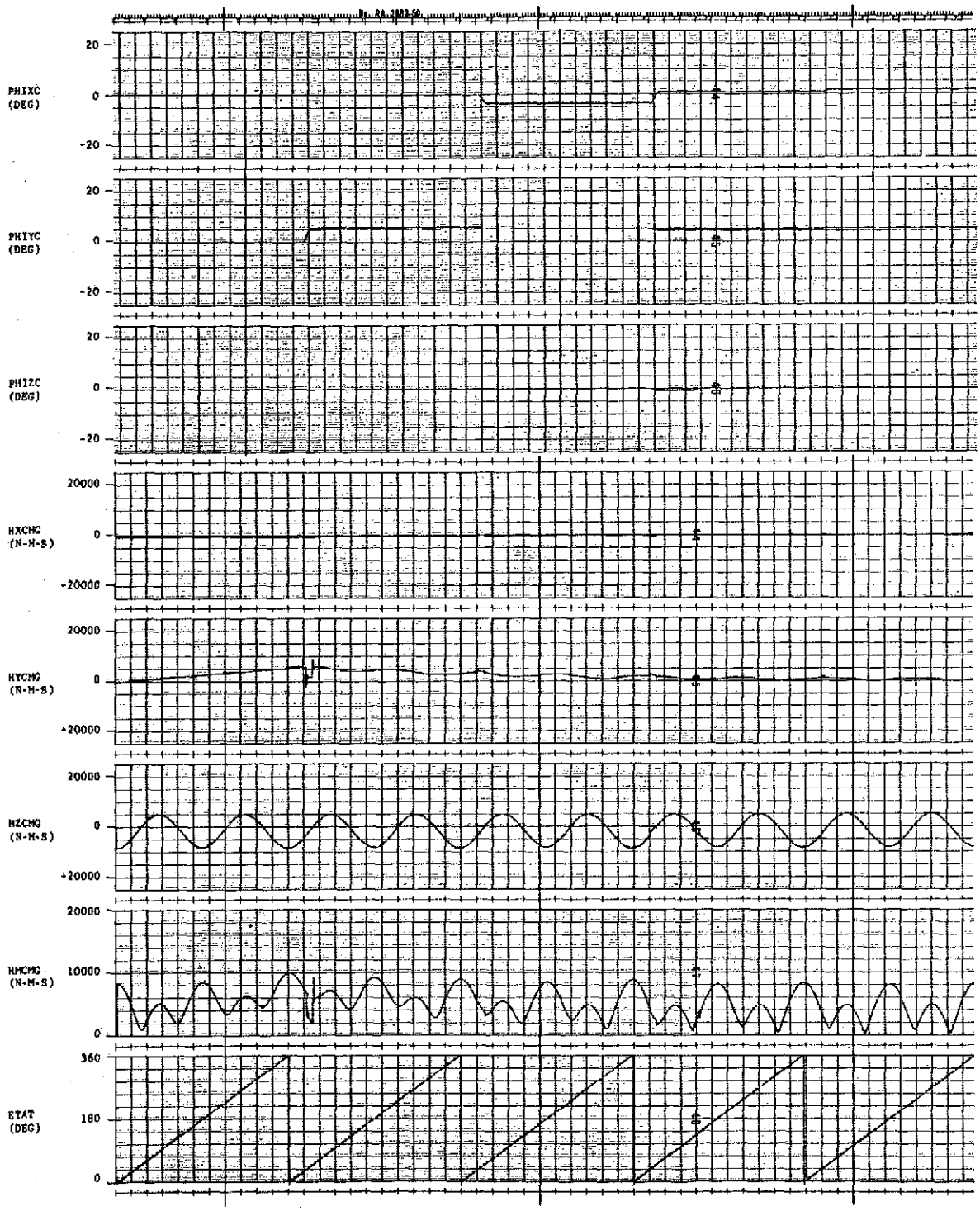

Figure 20. Z-POP, T_{YBD} = 1.0 N-m.

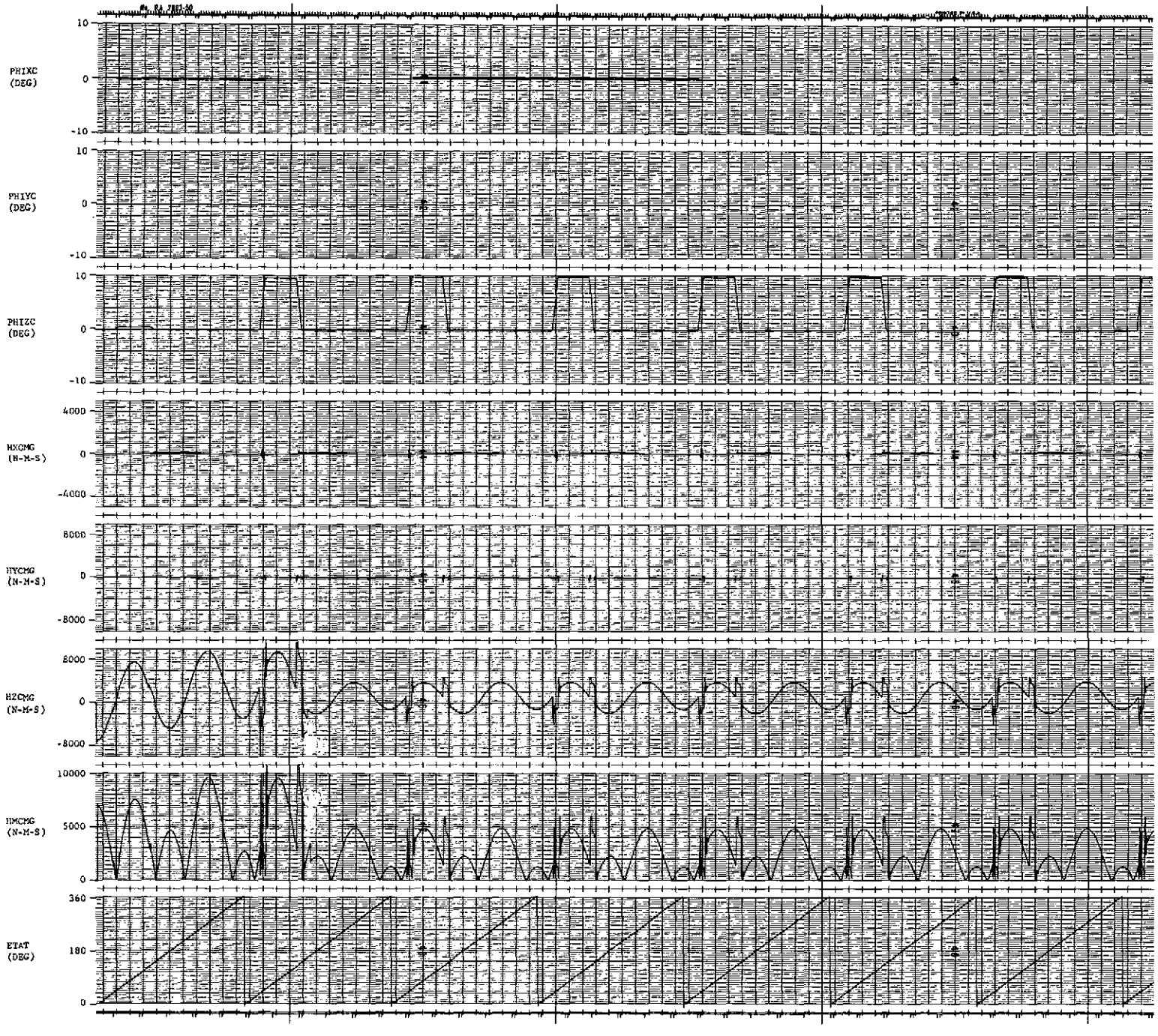

Figure 21. Z-POP, T_{ZBD} = 0.8 N-m.

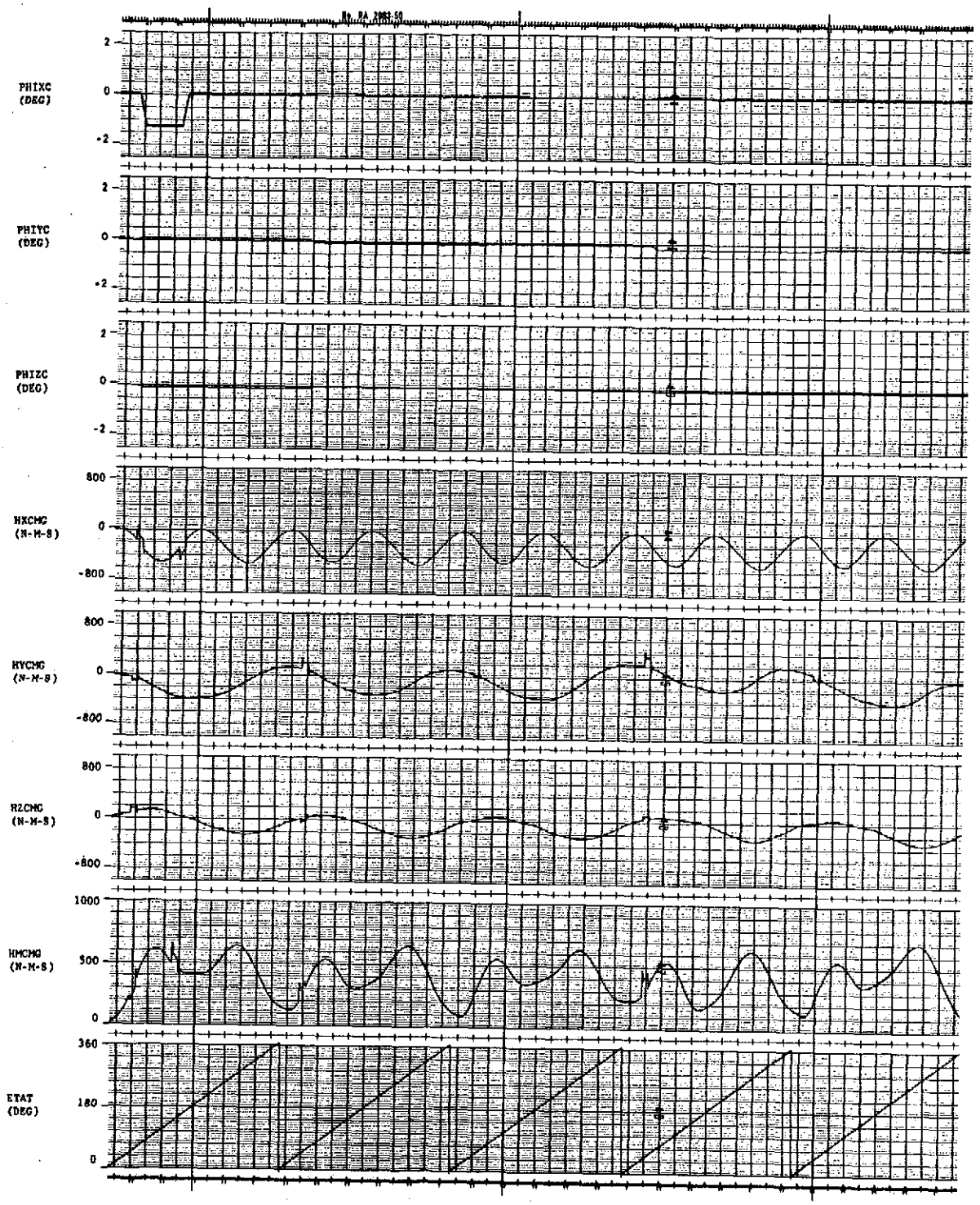

Figure 22. X-POP, T. A. No. 1 at T_S = 14 000 sec.

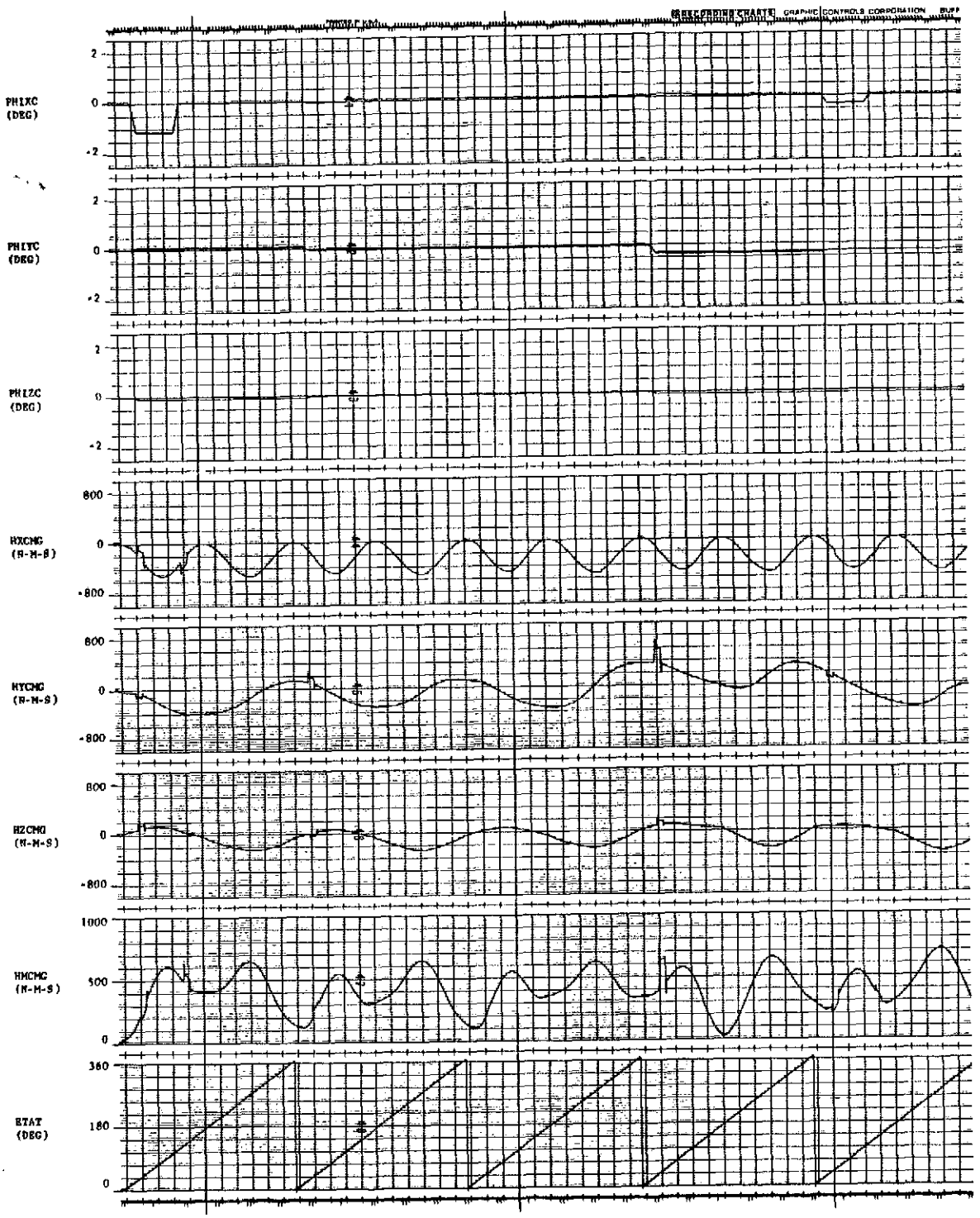

Figure 23. X-POP, T.A. No. 2 at T_S = 14 000 sec.

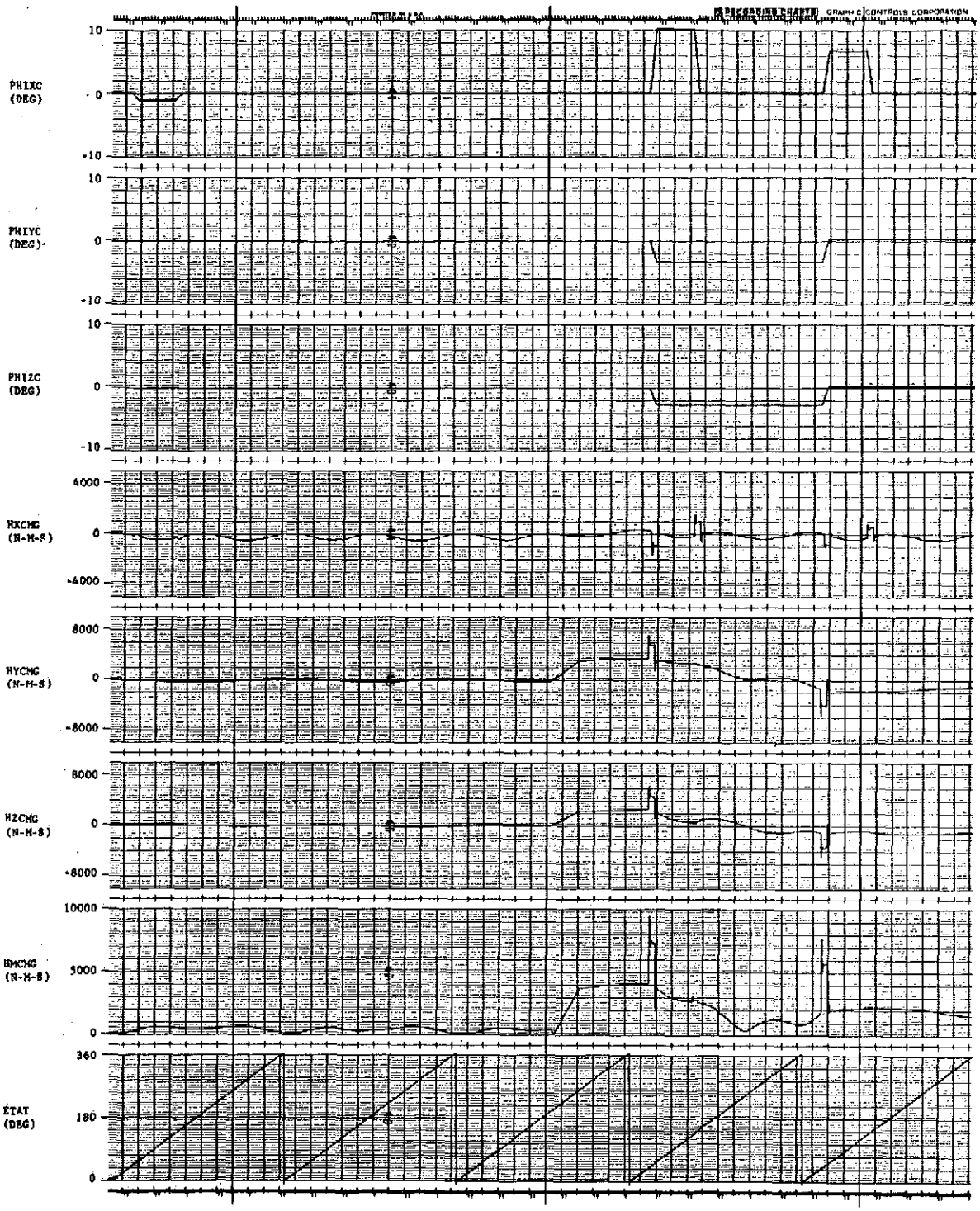

Figure 24. X-POP, LBNP at T_S = 14 000 sec.

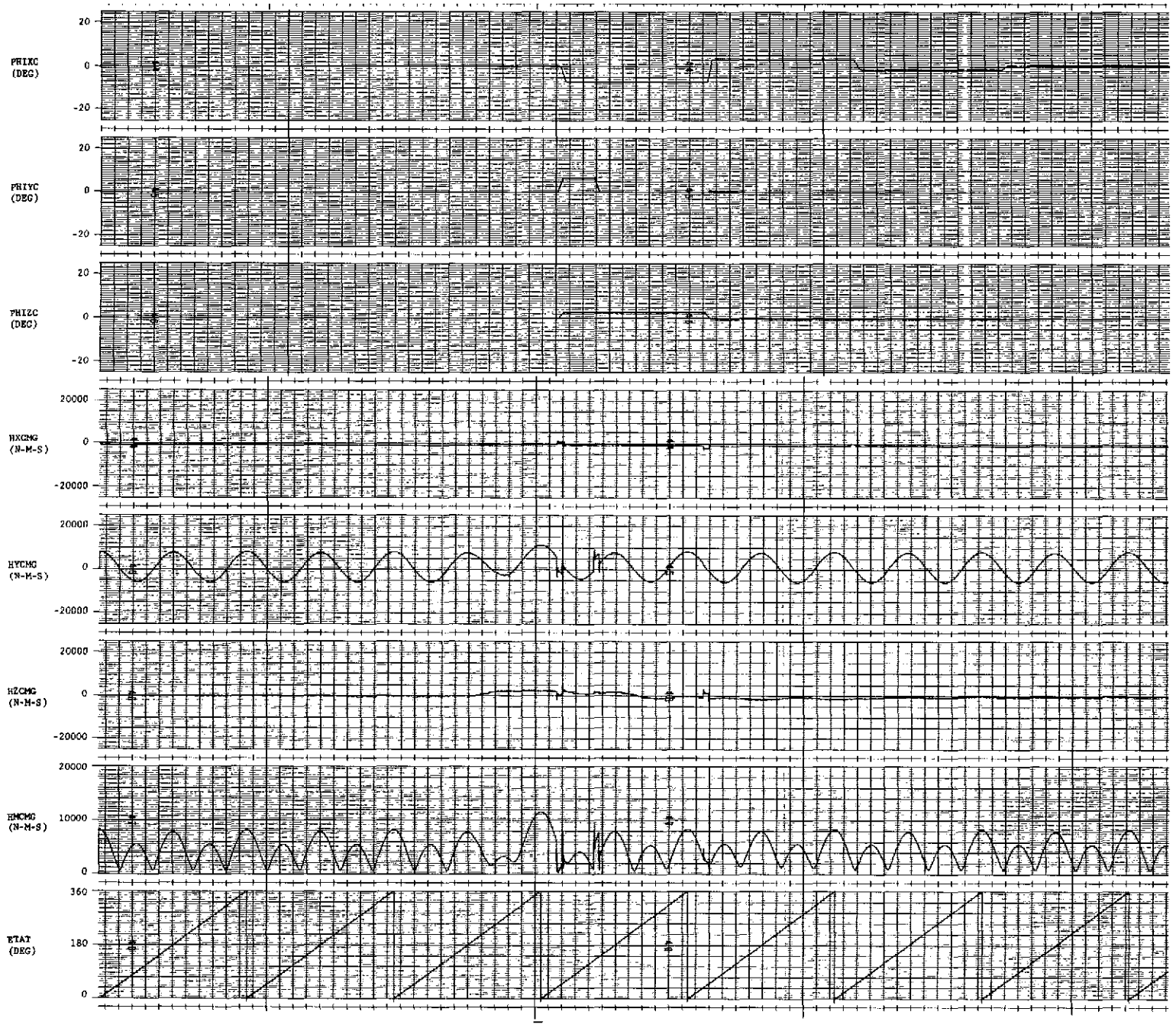

Figure 25. Y-POP, LBNP at T_S = 14 000 sec.

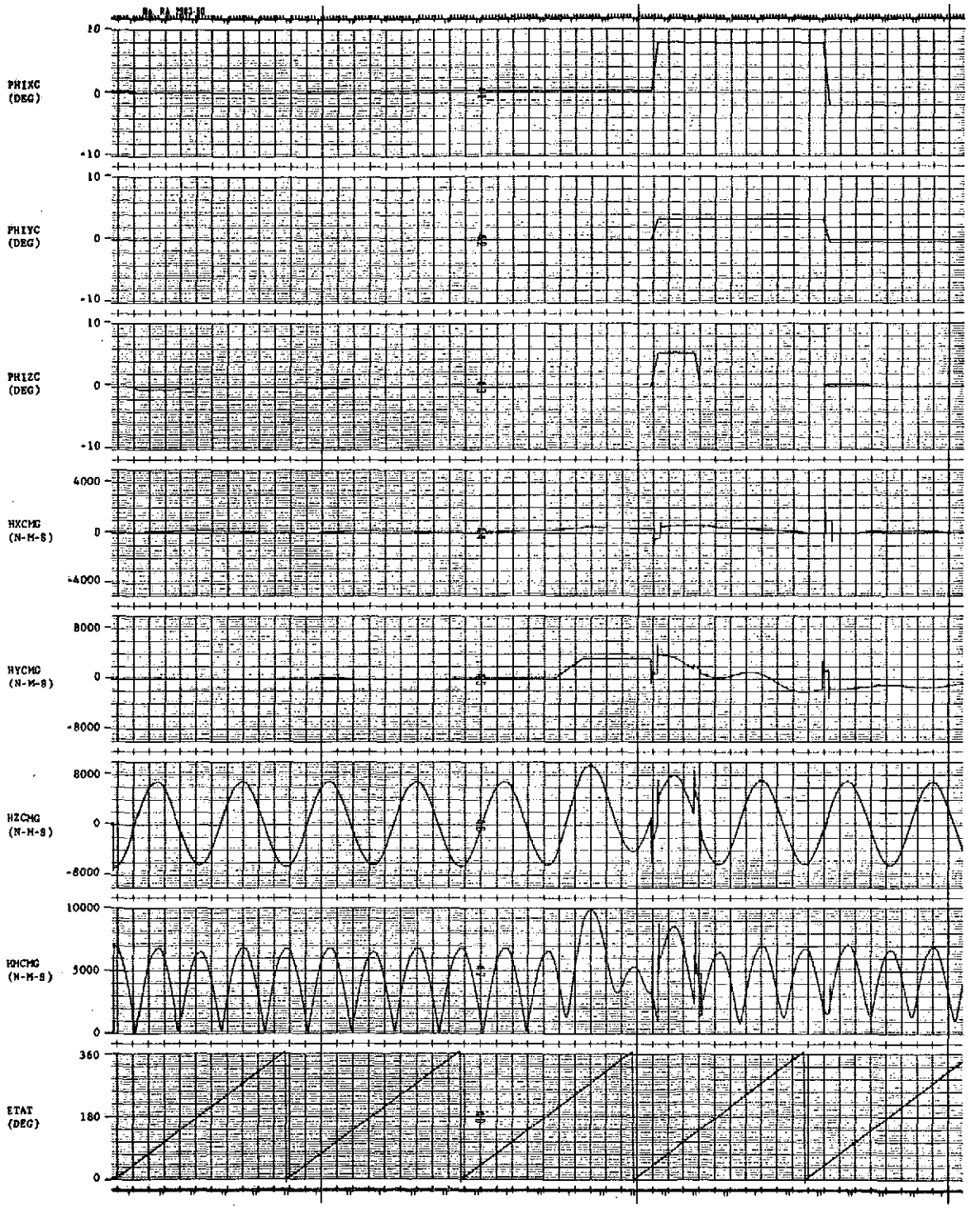

Figure 26. Z-POP, LBNP at T_S = 14 000 sec.

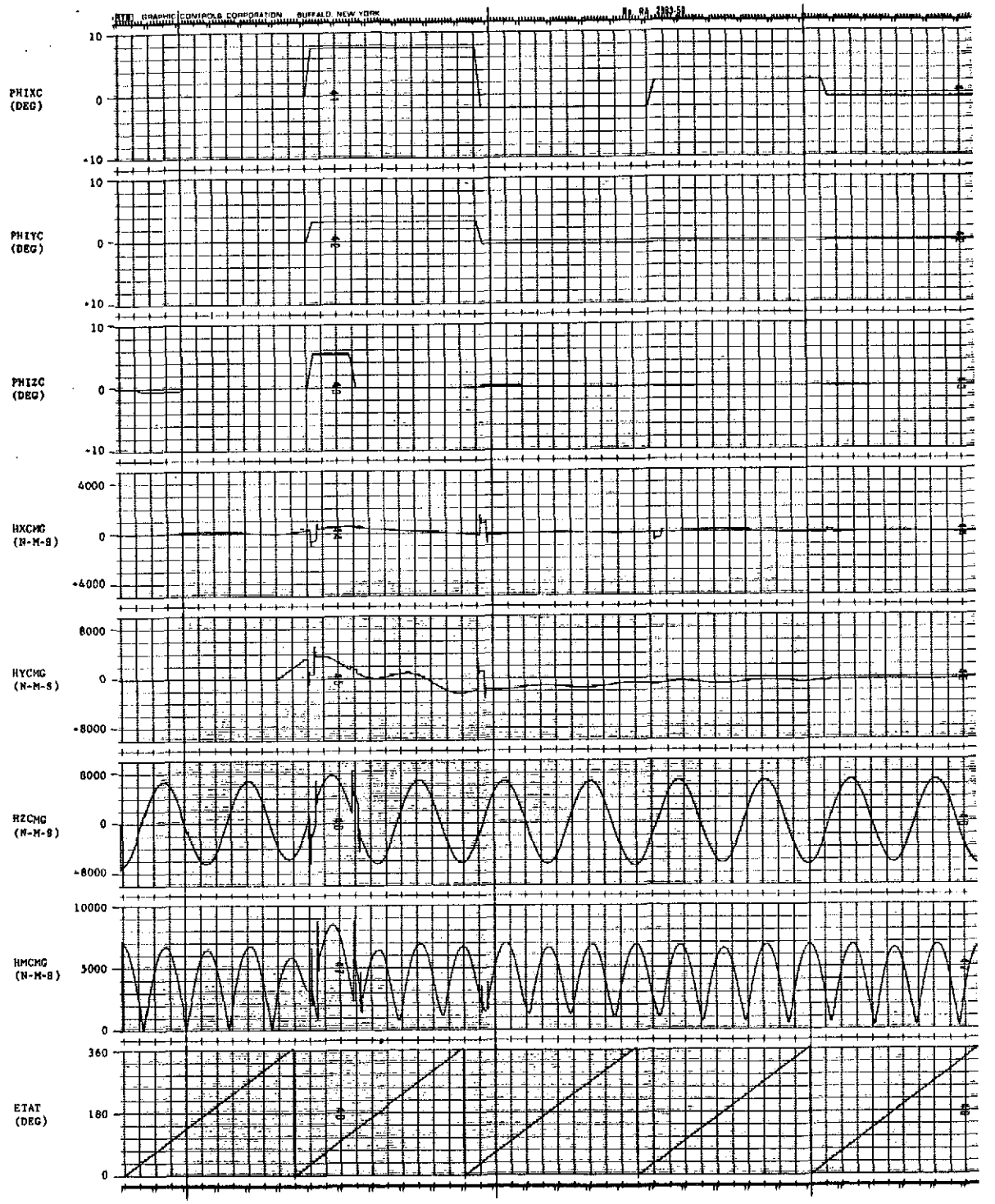

Figure 27. Z-POP, LBNP at T_S = 5100 sec.

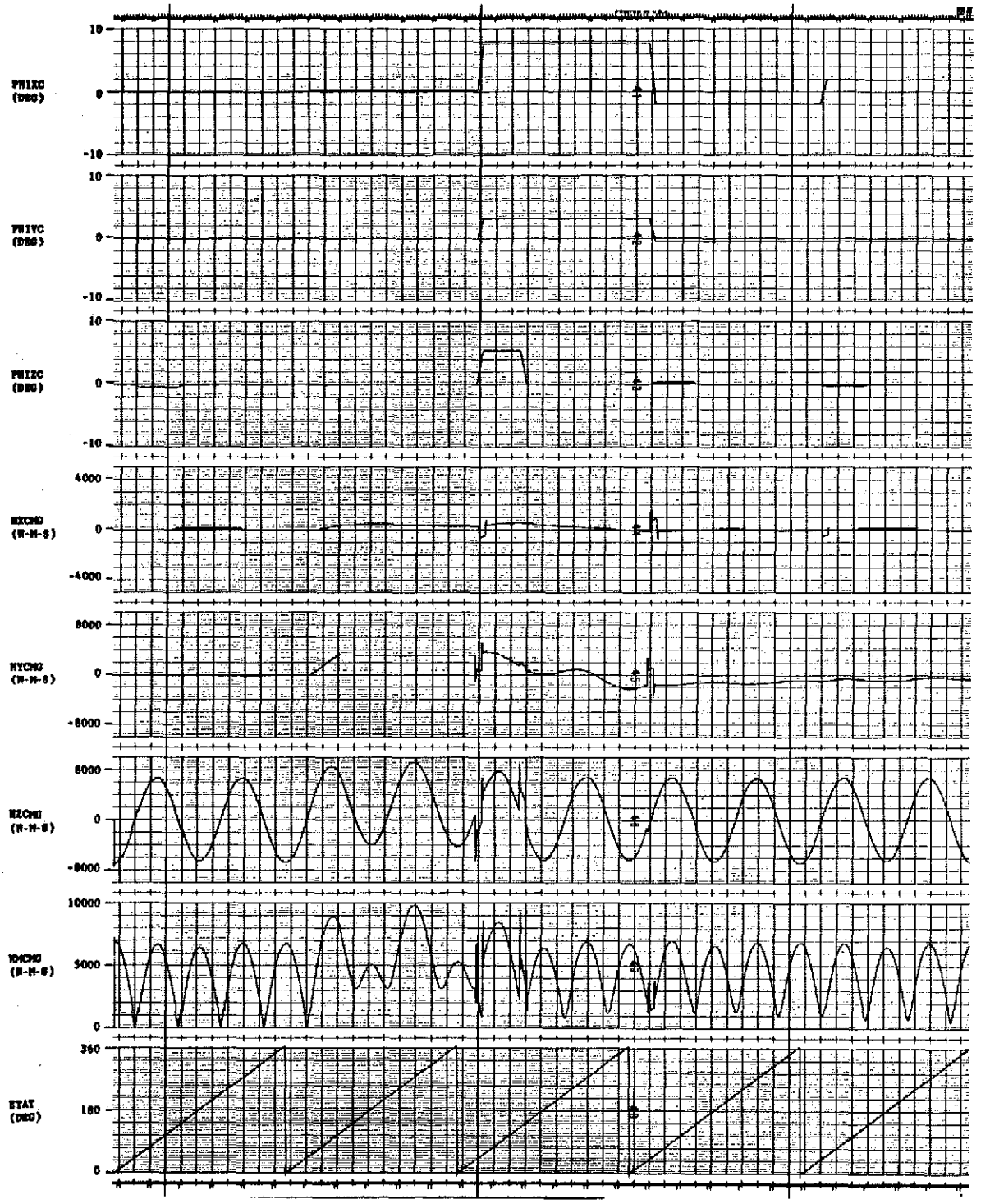

Figure 28. Z-POP, LBNP at T_S = 6300 sec.

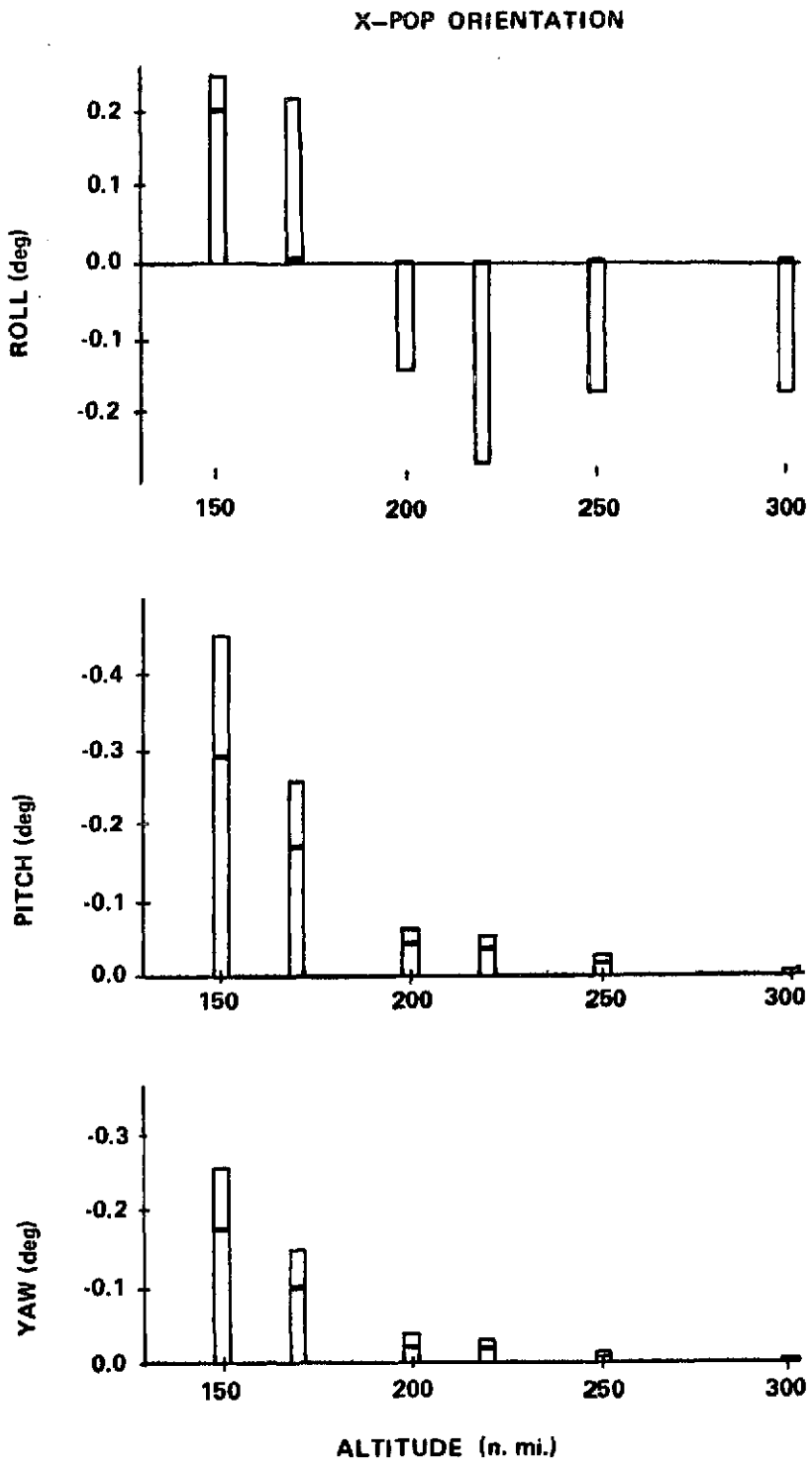

Figure 29. X-POP, aerodynamic disturbance.

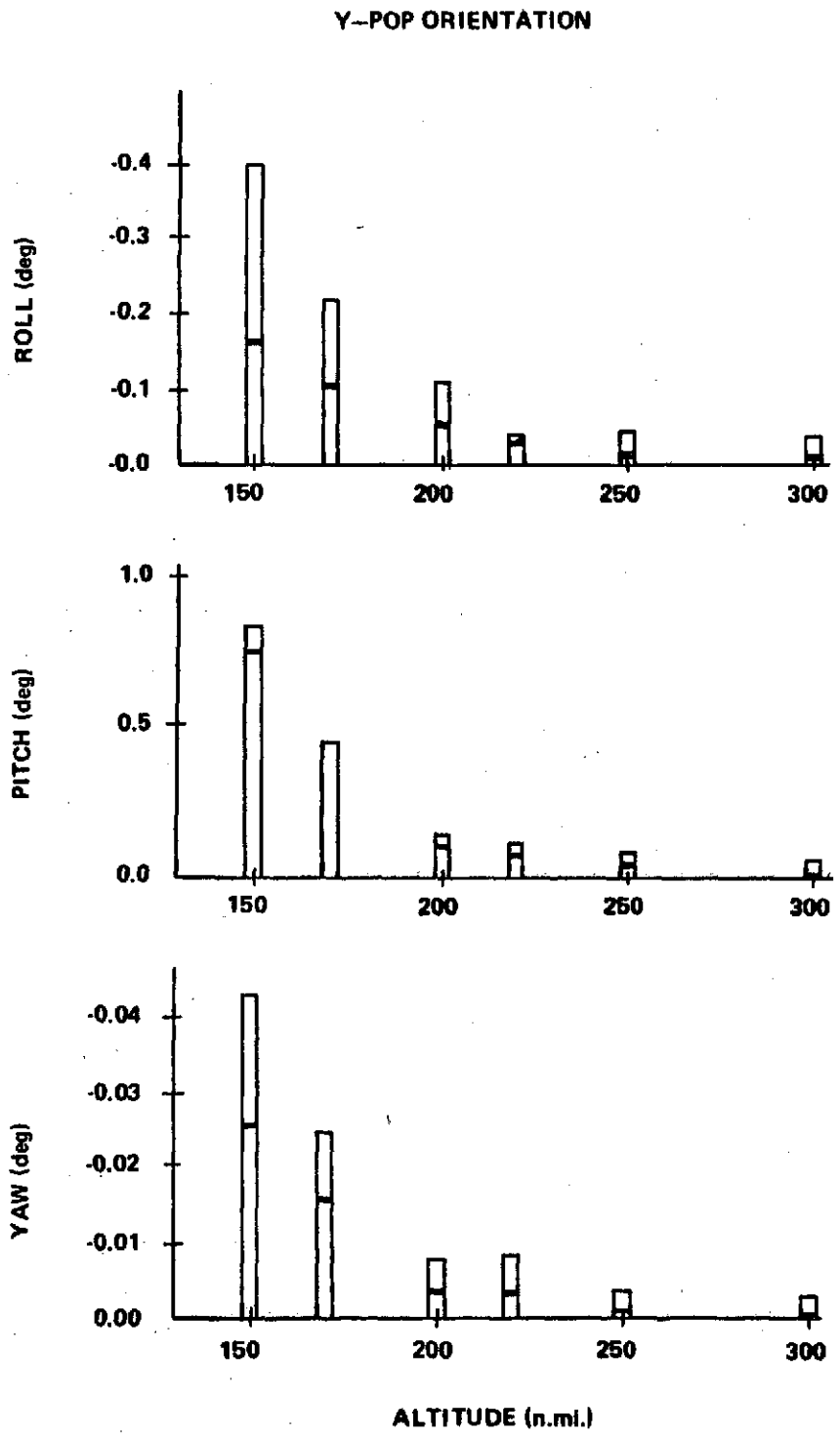

Figure 30. Y-POP, aerodynamic disturbance.

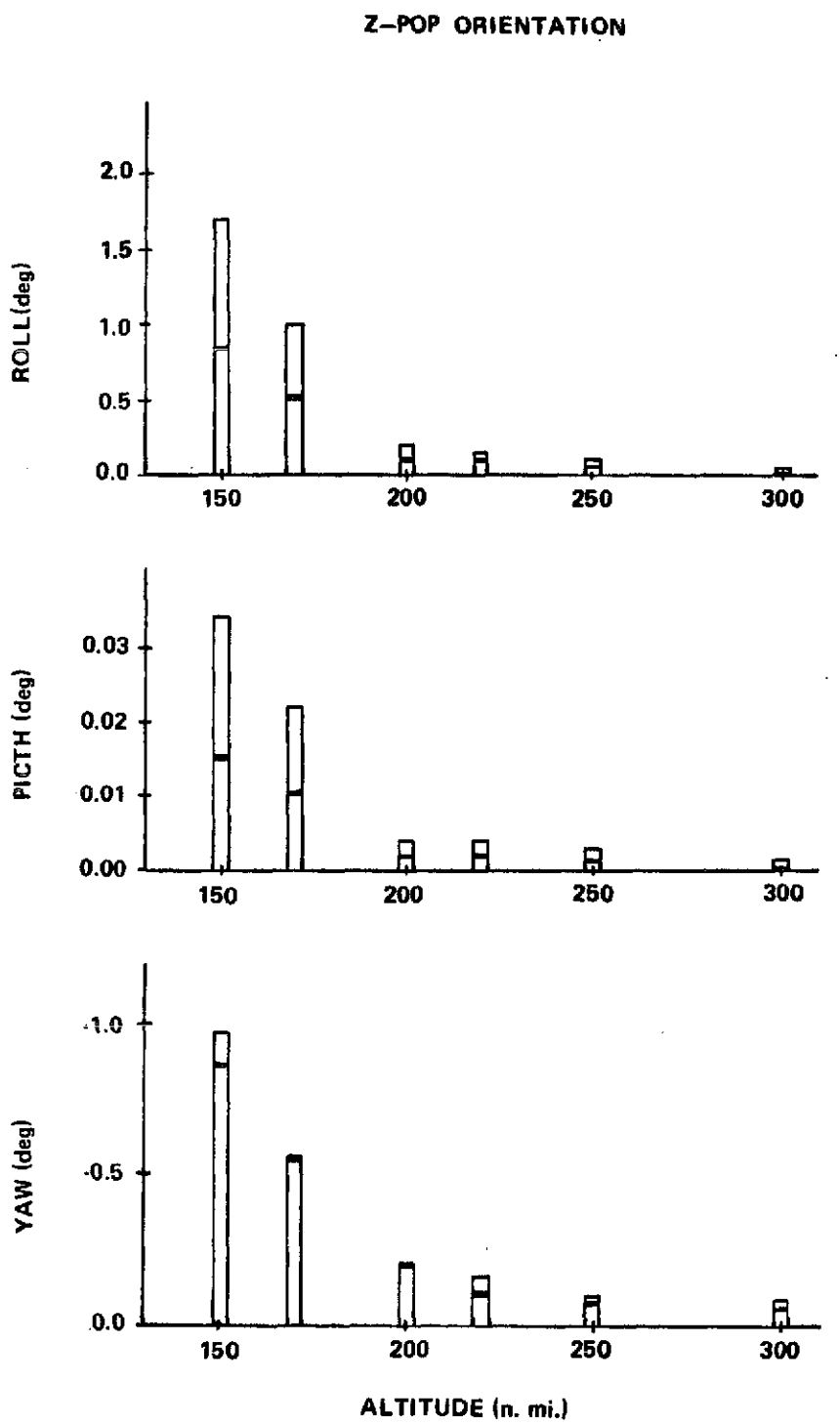

Figure 31. Z-POP, aerodynamic disturbance.

APPENDIX

DERIVATION OF DUMPING SCHEME EQUATIONS

A. Gravity Gradient Torque

The gravity gradient torque can be expressed in the vector-dyadic form,

$$\overline{T}_{GG} = 3\omega_o^2 \, \tilde{r}\bar{I}\bar{r} \quad . \tag{A-1}$$

When the vehicle axes are principal axes of inertia, then equation (A-1) can be expressed in the matrix form,

$$\begin{Bmatrix} T_{GG_1} \\ T_{GG_2} \\ T_{GG_3} \end{Bmatrix}^P = 3\omega_o^2 \begin{Bmatrix} (I_3 - I_2) & r_2 & r_3 \\ (I_1 - I_3) & r_3 & r_1 \\ (I_2 - I_1) & r_1 & r_2 \end{Bmatrix} \quad . \tag{A-2}$$

In principal axes for X-POP,

$$\begin{Bmatrix} T_{GG_1} \\ T_{GG_2} \\ T_{GG_3} \end{Bmatrix}^P \cong \frac{3}{2} \omega_o^2 \begin{Bmatrix} I_{\Delta 1}(S2\theta - 2\epsilon_1 C2\theta) \\ I_{\Delta 2}(\epsilon_2 + \epsilon_2 C2\theta + \epsilon_3 S2\theta) \\ I_{\Delta 3}(-\epsilon_3 + \epsilon_3 C2\theta - \epsilon_2 S2\theta) \end{Bmatrix} \quad ; \tag{A-3}$$

Y-POP,

$$\begin{Bmatrix} T_{GG_1} \\ T_{GG_2} \\ T_{GG_3} \end{Bmatrix}^P \cong \frac{3}{2} \omega_o^2 \begin{Bmatrix} I_{\Delta 1}(-\epsilon_1 - \epsilon_1 C2\theta + \epsilon_3 S2\theta) \\ I_{\Delta 2}(-S2\theta + 2\epsilon_2 C2\theta) \\ I_{\Delta 3}(\epsilon_3 - \epsilon_3 C2\theta - \epsilon_1 S2\theta) \end{Bmatrix} \quad ; \tag{A-4}$$

Z-POP,

$$\begin{Bmatrix} T_{GG_1} \\ T_{GG_2} \\ T_{GG_3} \end{Bmatrix}^P \cong \frac{3}{2}\,\omega_o^2 \begin{Bmatrix} I_{\Delta 1}(\epsilon_1 + \epsilon_1\, C2\theta - \epsilon_2\, S2\theta) \\ I_{\Delta 2}(-\epsilon_2 + \epsilon_2\, C2\theta + \epsilon_1\, S2\theta) \\ I_{\Delta 3}(-S2\theta - 2\epsilon_3\, C2\theta) \end{Bmatrix} . \qquad (A\text{-}5)$$

B. Momentum Dumping of In-Plane Axes

A small rotation about an essentially in-plane axis produces a change in the bias torque about that axis which can be used as a control torque to dump accumulated momentum from the same axis of the CMG control system. The average torque capability available per orbit for momentum dumping can be expressed as,

$$T_{GD_{ij}} = \hat{T}_{GG_{ij}} = \frac{1}{T_o} \int_0^{T_o} T_{GG_{ij}}\, dt \quad , \qquad (A\text{-}6)$$

where

$T_{GD_{ij}}$ is the gravity gradient dump torque capability

i is the POP orientation

j is the component label in the principal vehicle frame

T_o is the orbital period.

The gravity gradient torque capability can be expressed as:

X-POP,

$$\begin{bmatrix} T_{GD_1} \\ T_{GD_2} \\ T_{GD_3} \end{bmatrix} \cong \frac{3}{2}\,\omega_o^2 \begin{bmatrix} 0 & \\ I_{\Delta 2} & \epsilon_2 \\ -I_{\Delta 3} & \epsilon_3 \end{bmatrix} \quad ; \tag{A-7}$$

Y-POP,

$$\begin{bmatrix} T_{GD_1} \\ T_{GD_2} \\ T_{GD_3} \end{bmatrix} \cong \frac{3}{2}\,\omega_o^2 \begin{bmatrix} -I_{\Delta 1} & \epsilon_1 \\ 0 & \\ I_{\Delta 3} & \epsilon_3 \end{bmatrix} \quad ; \tag{A-8}$$

Z-POP,

$$\begin{bmatrix} T_{GD_1} \\ T_{GD_2} \\ T_{GD_3} \end{bmatrix} \cong \frac{3}{2}\,\omega_o^2 \begin{bmatrix} I_{\Delta 1} & \epsilon_1 \\ -I_{\Delta 2} & \epsilon_2 \\ 0 & \end{bmatrix} \quad . \tag{A-9}$$

During the time that the vehicle is held in an inertial hold, the gravity gradient dump torque is a constant. The momentum dumping capability can then be calculated by

$$H_D = T_{GD} \cdot \Delta t \quad , \tag{A-10}$$

where Δt is the time interval of constant attitude. For an orbit,

$$\Delta t = T_o = \frac{2\pi}{\omega_o} \quad , \tag{A-11}$$

and the momentum dumping capability per orbit is then

$$H_D = \frac{2\pi}{\omega_o} T_{GD} \quad . \tag{A-12}$$

Using equation (A-7), the momentum dumping capability [equation (A-12)] for a vehicle referenced to either an X-POP, Y-POP, or Z-POP orientation can be expressed in matrix form as:

X-POP,

$$\begin{bmatrix} H_{D_1} \\ H_{D_2} \\ H_{D_3} \end{bmatrix} \cong 3\pi\omega_o \begin{bmatrix} 0 & \\ I_{\Delta 2} & \epsilon_2 \\ -I_{\Delta 3} & \epsilon_3 \end{bmatrix} \quad ; \tag{A-13}$$

Y-POP,

$$\begin{bmatrix} H_{D_1} \\ H_{D_2} \\ H_{D_3} \end{bmatrix} \cong 3\pi\omega_o \begin{bmatrix} -I_{\Delta 1} & \epsilon_1 \\ 0 & \\ I_{\Delta 3} & \epsilon_3 \end{bmatrix} \quad ; \tag{A-14}$$

Z-POP,

$$\begin{bmatrix} H_{D_1} \\ H_{D_2} \\ H_{D_3} \end{bmatrix} \cong 3\pi\omega_o \begin{bmatrix} I_{\Delta 1} & \epsilon_1 \\ -I_{\Delta 2} & \epsilon_2 \\ 0 & \end{bmatrix} \quad . \tag{A-15}$$

The momentum dumping capability for the in-plane axes [equations (A-13), (A-14), and (A-15)] indicates the amount of momentum which can be dumped from the in-plane axes over an entire orbital period.

C. Momentum Dumping of POP Axes

A "single" small rotation about the vehicle in-plane axes held constant over the orbital period will not provide a bias torque on the POP axis. However, a "pair" of small rotations about the vehicle POP axis when properly executed (timed) will result in a bias gravity gradient torque on that axis which can be used as a control torque to dump accumulated momentum from the same axis of the CMG control system.

The gravity gradient torque equations in principal axes can be expressed as:

X-POP,

$$\begin{Bmatrix} T_{GG_1} \\ T_{GG_2} \\ T_{GG_3} \end{Bmatrix}^P \cong \frac{3}{2}\,\omega_o^2 \begin{Bmatrix} I_{\Delta 1} & S2(\theta - \epsilon_1) \\ I_{\Delta 2} & - - - \\ I_{\Delta 3} & - - - \end{Bmatrix} ; \qquad (A-16)$$

Y-POP,

$$\begin{Bmatrix} T_{GG_1} \\ T_{GG_2} \\ T_{GG_3} \end{Bmatrix}^P \cong \frac{3}{2}\,\omega_o^2 \begin{Bmatrix} I_{\Delta 1} & - - - \\ -I_{\Delta 2} & S2(\theta - \epsilon_2) \\ I_{\Delta 3} & - - - \end{Bmatrix} ; \qquad (A-17)$$

Z-POP,

$$\begin{Bmatrix} T_{GG_1} \\ T_{GG_2} \\ T_{GG_3} \end{Bmatrix}^P \cong \frac{3}{2}\,\omega_o^2 \begin{Bmatrix} I_{\Delta 1} & - - - \\ I_{\Delta 2} & - - - \\ -I_{\Delta 3} & S2(\theta + \epsilon_3) \end{Bmatrix} . \qquad (A-18)$$

A pair of properly timed rotations (changes in ϵ_1, ϵ_2, or ϵ_3) effects a bias torque by altering the shape of the gravity gradient torque profile from the symmetric sinusoid, characteristic of a vehicle inertially held in a POP orientation. The type of paired rotation maneuver utilized was the position/position maneuver.

D. Position/Position Maneuver

The gravity gradient torque on the POP axes [equations (A-12), (A-13), and (A-14)] as a result of the position/position maneuver is of the form

$$T_{GG_{ij}} = \frac{3}{2} \omega_o^2 I_{\Delta j} \sin 2(\theta - \epsilon_j) \quad , \quad i = j \quad , \tag{A-19}$$

where

i is the POP orientation label

j is the component label in the principal vehicle frame

and

$\epsilon_j = 0$ for $t_0 \leq t < t_1$ and $t_2 < t \leq T_o$

$\epsilon_j =$ a constant for $t_1 \leq t \leq t_2$.

The average torque capability over an orbit for momentum dumping on a POP axis is

$$T_{GD_{ij}} = \frac{1}{T_o} \int_0^{T_o} T_{GG_{ij}} \, dt \quad , \quad i = j$$

$$= \frac{3\omega_o^2}{2T_o} I_{\Delta j} \int_0^{T_o} \sin 2(\theta - \epsilon_j) \, dt$$

$$= \frac{3\omega_o^3}{4\pi} I_{\Delta j} \left\{ \int_{t_0}^{t_1} \sin 2\theta \, dt + \int_{t_1}^{t_2} \sin 2(\theta - \epsilon_j) \, dt + \int_{t_2}^{T_o} \sin 2\theta \, d\theta \right\}$$

$$= \frac{3\omega_o^2}{4\pi} I_{\Delta j} \left\{ \int_{\theta_0}^{\theta_1} \sin 2\theta \, d\theta + \int_{\theta_1}^{\theta_2} \sin 2(\theta - \epsilon_j) \, d\theta + \int_{\theta_2}^{2\pi} \sin 2\theta \, d\theta \right\}$$

or

$$T_{GD_{ij}} = \frac{3\omega_o^2}{4\pi} I_{\Delta j} \left\{ 4 \int_0^{\epsilon_j/2} \cos 2\theta \, d\theta \right\} \quad . \tag{A-20}$$

Thus,

$$T_{GD_{ij}} = \frac{3\omega_o^2}{2\pi} I_{\Delta j} \sin \epsilon_j \quad , \quad i = j \quad ,$$

or (A-21)

$$T_{GD_{ij}} = \frac{3\omega_o^2}{2\pi} I_{\Delta j} \epsilon_j \quad ,$$

or in matrix form as

$$\begin{Bmatrix} T_{GD_{11}} \\ T_{GD_{22}} \\ T_{GD_{33}} \end{Bmatrix} \cong \frac{3\omega_o^2}{2\pi} \begin{Bmatrix} I_{\Delta 1} & \epsilon_1 \\ -I_{\Delta 2} & \epsilon_2 \\ -I_{\Delta 3} & \epsilon_3 \end{Bmatrix} \quad . \tag{A-22}$$

The momentum dumping capability per orbit on the POP axis is then given by

$$H_{D_{ij}} = T_{GD_{ij}} T_o \quad , \quad i = j \tag{A-23}$$

or

$$H_{D_{ij}} \cong 3\omega_o I_{\Delta j} \epsilon_j \quad , \quad i = j \quad . \tag{A-24}$$

The momentum dumping capability (H_D) per orbit for the POP axis of a vehicle in either X-POP, Y-POP, or Z-POP orientation due to a small angle position/position maneuver can be summarized in matrix form as

$$\begin{Bmatrix} H_{D_{11}} \\ H_{D_{22}} \\ H_{D_{33}} \end{Bmatrix} \cong 3\omega_o \begin{Bmatrix} I_{\Delta 1} & \epsilon_1 \\ -I_{\Delta 2} & \epsilon_2 \\ -I_{\Delta 3} & \epsilon_3 \end{Bmatrix} \quad . \tag{A-25}$$

Equation (A-25) then can be written for:

X-POP,

$$\begin{Bmatrix} H_{D_{11}} \\ H_{D_{12}} \\ H_{D_{13}} \end{Bmatrix} \cong 3\pi\omega_o \begin{Bmatrix} I_{\Delta 1} & \epsilon_1/\pi \\ I_{\Delta 2} & \epsilon_2 \\ -I_{\Delta 3} & \epsilon_3 \end{Bmatrix} \quad ; \tag{A-26}$$

Y-POP,

$$\begin{Bmatrix} H_{D_{21}} \\ H_{D_{22}} \\ H_{D_{23}} \end{Bmatrix} \cong 3\pi\omega_o \begin{Bmatrix} -I_{\Delta 1} & \epsilon_1 \\ -I_{\Delta 2} & \epsilon_2/\pi \\ I_{\Delta 3} & \epsilon_3 \end{Bmatrix} \quad ; \tag{A-27}$$

Z-POP,

$$\begin{Bmatrix} H_{D_{31}} \\ H_{D_{32}} \\ H_{D_{33}} \end{Bmatrix} \cong 3\pi\omega_o \begin{Bmatrix} I_{\Delta 1} & \epsilon_1 \\ -I_{\Delta 2} & \epsilon_2 \\ -I_{\Delta 3} & \epsilon_3/\pi \end{Bmatrix} . \qquad \text{(A-28)}$$

E. Momentum Dumping Scheme

Presented below are the momentum dumping scheme equations for the in-plane axes.

Initial input for the Nth orbit (normally N = 1) (Note: The end conditions of the (N-1) th orbit become the initial conditions for the Nth orbit.):

$\epsilon_{oj(N-1)}$

$H_{j(N-1)}$

H_{Cj}

$H_{AVj(N-1)}$

$H_{\epsilon j(N-1)} = H_{j(N-1)} - H_{Cj}$

K_{PDj} .

Beginning-of-orbit calculations for the Nth orbit:

$$H_{DCJ(N)} = -K_{PDj} H_{\epsilon j(N-1)}$$

$$\epsilon_{cj(N)} = \epsilon_{oj(N-1)} + \frac{H_{DCj(N)}}{K_{ij}} .$$

During-the-orbit calculations:

$$H_{AVj(N)} = \frac{1}{T_o} \int_{t(N-1)}^{t(N)} H_j \, dt \quad , \quad t \text{ is measured from } \theta_D \text{ to } \theta_D + 2\pi \quad .$$

End-of-orbit calculations:

$$H_{SECj(N)} = H_{AVj(N)} - H_{AVj(N-1)}$$

$$\epsilon_{oj(N)} = \epsilon_{cj(N)} - \frac{H_{SECj(N)}}{K_{ij}}$$

$$H_{\epsilon j(N)} = H_{j(N)} - H_{Cj} \quad .$$

For the POP axes, the momentum dumping scheme equations are as follows:

Initial input for the Nth orbit (normally N = 1):

$$H_{j(N-1)}$$

$$H_{Cj}$$

$$H_{\epsilon j(N-1)} = H_{j(N-1)} - H_{Cj}$$

$$K_{PDj} \quad .$$

Beginning-of-orbit calculations for the Nth orbit:

$$H_{DCj(N)} = -K_{PDj} H_{\epsilon j(N-1)}$$

$$\epsilon_{cj(N)} = \frac{H_{DCj(N)}}{K_{ij}}$$

$$\epsilon_j = \epsilon_{cj(N)} \quad .$$

End-of-orbit calculations:

$$H_{\epsilon j(N)} = H_{j(N)} - H_{Cj}$$

Test for the sign of $H_{\epsilon j(N)}$:

$$\text{for } H_{\epsilon j(N)} \begin{cases} <0, \text{ set } m_j = 1 \\ >0, \text{ set } m_j = 2 \end{cases}$$

F. Flow Chart

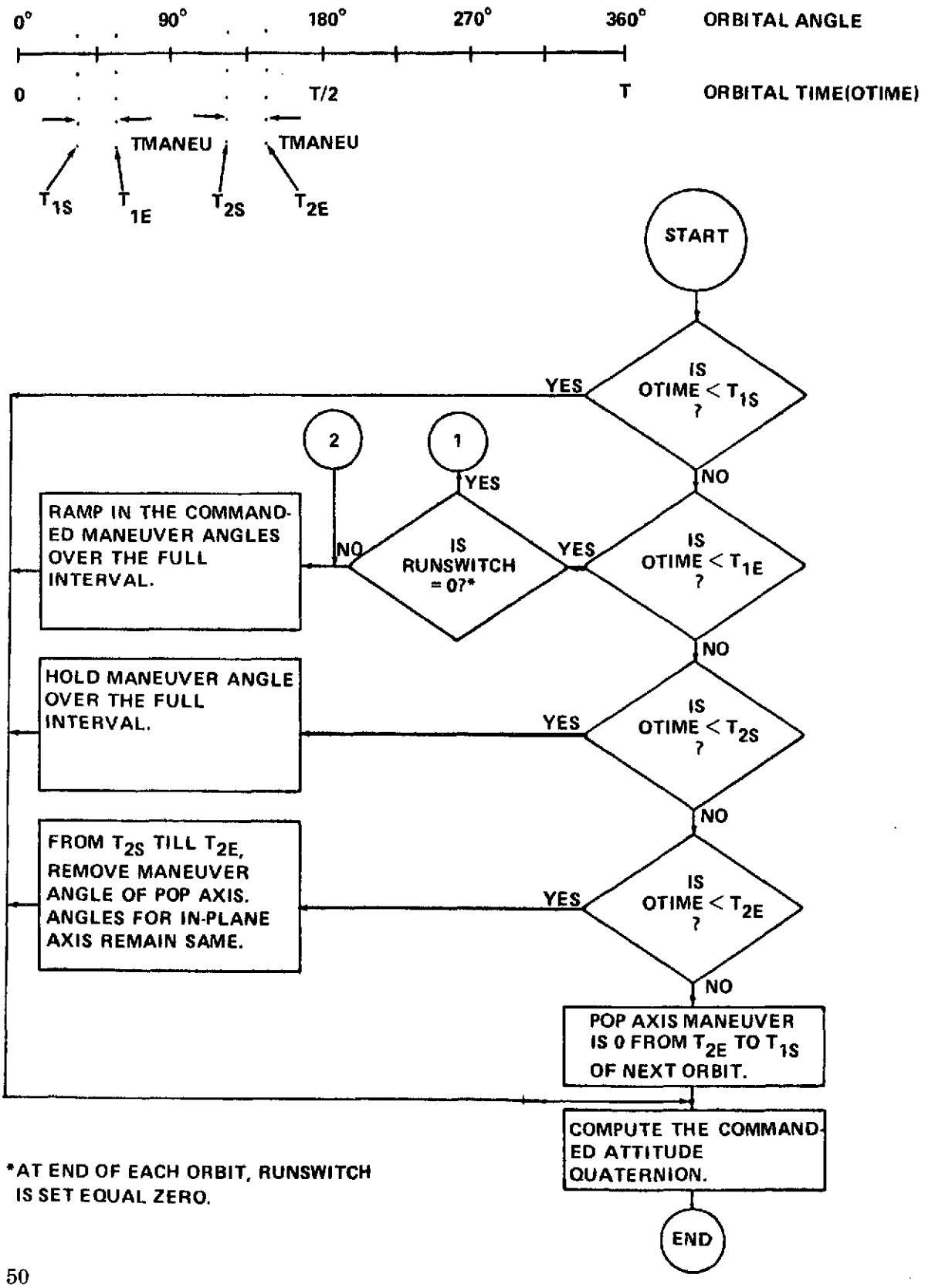

*AT END OF EACH ORBIT, RUNSWITCH IS SET EQUAL ZERO.

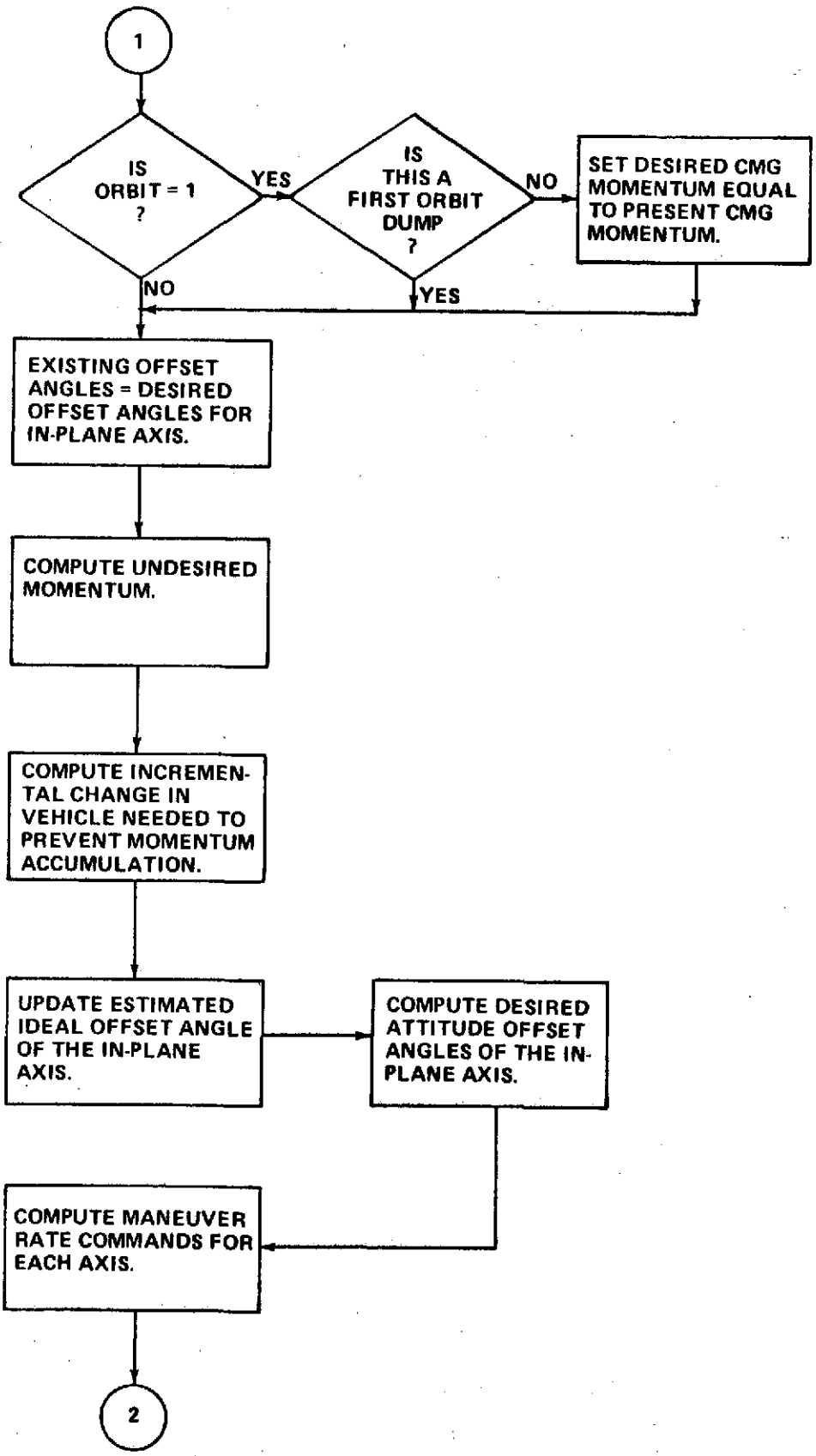
1
IS ORBIT = 1 ?
YES
IS THIS A FIRST ORBIT DUMP ?
NO
SET DESIRED CMG MOMENTUM EQUAL TO PRESENT CMG MOMENTUM.
NO
YES
EXISTING OFFSET ANGLES = DESIRED OFFSET ANGLES FOR IN-PLANE AXIS.
COMPUTE UNDESIRED MOMENTUM.
COMPUTE INCREMENTAL CHANGE IN VEHICLE NEEDED TO PREVENT MOMENTUM ACCUMULATION.
UPDATE ESTIMATED IDEAL OFFSET ANGLE OF THE IN-PLANE AXIS.
COMPUTE DESIRED ATTITUDE OFFSET ANGLES OF THE IN-PLANE AXIS.
COMPUTE MANEUVER RATE COMMANDS FOR EACH AXIS.
2

APPROVAL

ORBITER/SPACELAB MOMENTUM MANAGEMENT FOR POP ORIENTATIONS

By Jerry W. Cox

The information in this report has been reviewed for security classification. Review of any information concerning Department of Defense or Atomic Energy Commission programs has been made by the MSFC Security Classification Offier. This report, in its entirety, has been determined to be unclassified.

This document has also been reviewed and approved for technical accuracy.

JAMES C. BLAIR
Chief, Control Systems Division

for J. A. LOVINGOOD
Director, Systems Dynamics Laboratory

☆ U.S. GOVERNMENT PRINTING OFFICE 1974 — 640-446 / 94 REGION NO. 4

DISTRIBUTION

INTERNAL

Director
DA01/Dr. Lucas

S&E-Systems Dynamics
ED01/Dr. Lovingood
ED01/Dr. Worley
ED11/Dr. Blair
ED11/Mr. Scofield
ED11/Mr. Borelli
ED15/Mr. Rheinfurth
ED15/Mr. Hall
ED15/Mr. Cox (15)
ED12/Dr. Seltzer
ED12/Mr. Buchanan
ED12/Mr. McNiel
ED12/Mr. Hammer
ED12/Mr. Shelton
ED12/Dr. Glaese
ED12/Mr. Kennel
ED13/Mr. Lewis
ED21/Mr. Ryan

S&E-Data Systems
EF24/Mr. Brooks
EF32/Mr. Teague

S&E-Systems Analysis & Integration
EL21/Mr. Lindberg
EL31/Mr. Palaoro
EL31/Mr. Currie
E132/Mr. Beam
EL33/Mr. Thrower
EL51/Mr. Deaton
EL51/Mr. Tanner
EL54/Mr. Polites
EL54/Mr. Chubb
EL54/Mr. Smith

S&E-Assoc. Dir. for Engineering
EE41/Mr. Hagood
EE41/Mr. Noel

S&E-Research & Technology Office
ER01/Mr. Sims

Spacelab Program Office
NA01/Mr. Lee
NA21/Mr. DeSanctis
NA31/Mr. Powell
NA31/Mr. Compton
NA41/Mr. Hoodless
NA41/Mr. Howard

AS61 (2)

AS61L (8)

CC01

AT01 (6)

EXTERNAL

Scientific and Technical Information
Facility (25)
P. O. Box 33
College Park, Md. 20740
Attn: NASA Representative (S-AK/RKT)

Martin Marietta Aerospace
Denver, Col. 80201
Attn: Mr. Cloud